



Available online at www.sciencedirect.com

ScienceDirect

Cosmochimica Acta

Geochimica et Cosmochimica Acta 203 (2017) 175-200

www.elsevier.com/locate/gca

Geochimica et

Early diagenesis and trace element accumulation in North American Arctic margin sediments

Zou Zou A. Kuzyk a,*, Charles Gobeil b, Miguel A. Goñi c, Robie W. Macdonald a,d

^a Centre for Earth Observation Science, Wallace Building, 125 Dysart Rd., University of Manitoba, Winnipeg, Manitoba R3T 2N2, Canada
 ^b INRS-ETE, Université du Québec, 490 de la Couronne, Québec, QC G1K 9A9, Canada
 ^c College of Earth, Ocean and Atmospheric Sciences, Oregon State University, 104 CEOAS Admin. Bldg., Corvallis, OR 97331, USA
 ^d Department of Fisheries and Oceans, Institute of Ocean Sciences, PO Box 6000, Sidney, BC V8L 4B2, Canada

Received 21 August 2014; accepted in revised form 8 December 2016; Available online 18 December 2016

Abstract

Concentrations of redox-sensitive elements (S, Mn, Mo, U, Cd, Re) were analyzed in a set of 27 sediment cores collected along the North American Arctic margin (NAAM) from the North Bering Sea to Davis Strait via the Canadian Archipelago. Sedimentary distributions and accumulation rates of the elements were used to evaluate early diagenesis in sediments along this section and to estimate the importance of this margin as a sink for key elements in the polar and global oceans. Distributions of Mn, total S and reduced inorganic S demonstrated that diagenetic conditions and thus sedimentary carbon turnover in the NAAM is organized regionally: undetectable or very thin layers (<0.5 cm) of surface Mn enrichment occurred in the Bering-Chukchi shelves; thin layers (1-5 cm) of surface Mn enrichment occurred in Barrow Canyon and Lancaster Sound; and thick layers (5-20 cm) of surface Mn enrichment occurred in the Beaufort Shelf, Canadian Archipelago, and Davis Strait. Inventories of authigenic S below the Mn-rich layer decreased about fivefold from Bering-Chukchi shelf and Barrow Canyon to Lancaster Sound and more than ten-fold from Bering-Chukchi shelf to Beaufort Shelf, Canadian Archipelago and Davis Strait. The Mn. total S and reduced inorganic S distributions imply strong organic carbon (OC) flux and metabolism in the Bering-Chukchi shelves, lower aerobic OC metabolism in Barrow Canyon and Lancaster Sound, and deep O₂ penetration and much lower OC metabolism in the Beaufort Shelf, Canadian Archipelago, and Davis Strait. Accumulation rates of authigenic S, Mo, Cd, Re, and U displayed marked spatial variability along the NAAM reflecting the range in sedimentary redox conditions. Strong relationships between the accumulation rates and vertical carbon flux, estimated from regional primary production values and water depth at the coring sites, indicate that the primary driver in the regional patterns is the supply of labile carbon to the seabed. Thus, high primary production combined with a shallow water column (average 64 m) leads to high rates of authigenic trace element accumulation in sediments from the Bering-Chukchi shelves. High to moderate primary production combined with deep water (average 610 m) leads to moderate rates of authigenic trace element accumulation in sediments from Lancaster Sound. Low to very low primary production combined with moderate water depths (average 380 m) leads to low rates of authigenic trace element accumulation in sediments in the Beaufort Shelf, Davis Strait and Canadian Archipelago. Authigenic Mo accumulation rates show a significant relationship with vascular plant input to the sediments, implying that terrestrial organic matter contributes significantly to metabolism in Arctic margin sediments. Our results suggest that the broad and shallow shelf of the Chukchi Sea, which has high productivity sustained by imported nutrients, contributes disproportionately to global biogeochemical cycles.

© 2017 The Authors. Published by Elsevier Ltd. This is an open access article under the CC BY-NC-ND license (http://creativecommons.org/licenses/by-nc-nd/4.0/).

Keyword: Redox-sensitive elements

E-mail addresses: ZouZou.Kuzyk@umanitoba.ca (Z.A. Kuzyk), Charles.Gobeil@ete.inrs.ca (C. Gobeil), mgoni@coas.oregonstate.edu (M.A. Goñi), Robie.Macdonald@dfo-mpo.gc.ca (R.W. Macdonald).

^{*} Corresponding author.

1. INTRODUCTION

Continental margins are now recognized as disproportionately important in many global biogeochemical cycles (Liu et al., 2000a; Jeandel et al., 2011). Although they occupy less than 10% of the global ocean surface area and their waters contribute less than 0.5% of the ocean volume, almost 90% of new primary production takes place in continental margin areas (Chen et al., 2003). Continental margin sediments account for as much as 90% of the oceanic burial of organic carbon (Liu et al., 2010) and are the principal sites of pyrite sulphur burial formed during microbial oxidation of labile organic matter by sulphate reduction (Berner, 1970, 1984). Organic matter and sulphide burial in continental margin sediments represent the major sink terms in the oceanic budgets of a number of redoxsensitive trace elements, including Mo, U, and Cd (Berner, 1982; Rosenthal et al., 1995a; Dunk et al., 2002; McManus et al., 2006; Raiswell et al., 2006; Scott et al., 2008).

The Arctic Ocean is unique among the world's oceans in that the continental margin comprises more than onehalf (52.9%) of the total ocean area (Jakobsson, 2002). Indeed, the Arctic margin comprises about 10% of the total continental margin area in the global ocean. The massive Arctic continental shelves and slopes are, in large part, seasonally ice-free; compared to other ocean margins, they receive large river water inputs together with large inputs of terrestrial nutrients, sediment, and trace elements; and compared to the Arctic Ocean basins, they exhibit much greater sea-ice production, biological productivity, sediment resuspension, and deposition and regeneration of organic matter (Stein and Macdonald, 2004). Consequently, processes over the shelves play a dominant role in the Arctic Ocean carbon budget (Liu et al., 2000b; Chen et al., 2003; Macdonald et al., 2010). The large, relatively productive shelf areas juxtaposed with low particle-flux interior basins gives rise to a strong boundary-scavenging removal regime in the Arctic Ocean, which influences the dissolved concentrations of particlereactive elements, the distribution of sedimentary sinks, and the advective export to other ocean areas (Moran et al., 2005; Cai et al., 2010; Kuzyk et al., 2013). For example, scavenging and phytoplankton uptake over the large, productive shelves lower dissolved iron concentrations in Arctic Ocean surface waters on a wide scale and consequently the transport of iron to the North Atlantic, where it may impact nitrogen fixation (Klunder et al., 2012). Thus, it is now widely recognized that an emphasis on the shallow shelf and slope domains is critical to understanding elemental cycles within the Arctic Ocean as a whole (Stein and Macdonald, 2004; Carmack and Wassman, 2006). The Arctic margin appears to contribute significantly to the organic carbon cycle in the global ocean, but it remains unclear what the significance of these shelves is for other elemental cycles.

Although there are common features for all Arctic shelves (compared to shelves elsewhere) in terms of seasonal ice cover, large inputs from land and exchange at the shelf edge, each shelf is distinct in terms of quantity

and disposition of freshwater inputs, rates of sediment and terrestrial organic matter supply, size, water depth, source of saline water, ice production, physical-biological forcing and food webs (Chen et al., 2003; Carmack and Wassman, 2006). Even along the NAAM there is tremendous diversity among the shelves. Thus, a major criticism of our state of knowledge of the continental shelves of the Arctic has been that it is "too disciplinary, regional and fractured" (Carmack and Wassman, 2006), particularly in the face of the rapid, unprecedented changes associated with climate warming (IPCC, 2013). With continuing decreases in ice cover, annual primary production in the Arctic Ocean may increase as much as threefold (Arrigo et al., 2008, 2012). Inputs of terrestrial organic matter may also increase dramatically due to increases in river runoff (Shiklomanov and Shiklomanov, 2003), erosion of soils into rivers (Guo et al., 2012) and coastal erosion (Vonk et al., 2012), in part supported by widespread permafrost degradation (Lantuit et al., 2013). The effects of changes in marine and terrestrial carbon cycles on the biogeochemistry within the Arctic Ocean are much more difficult to predict (cf., Serreze et al., 2007; McGuire et al., 2009; Walsh et al., 2011; Doney et al., 2012; Macdonald et al., 2015a). Nevertheless, it is clear that a comprehensive understanding of baseline conditions prior to the changes consequent to the loss of sea ice and permafrost thaw is essential to detect the direction, magnitude and rates of biogeochemical changes in the Arctic Ocean (cf., Macdonald et al., 2015b).

One approach to studying carbon cycling that has yet to be applied to the Arctic continental margin is the investigation of the sedimentary distribution of redox-sensitive elements such as Cd, Re, U, and Mo (cf., Calvert and Pedersen, 1993; Crusius et al., 1996; Crusius and Thomson, 2000; Sundby et al., 2004; Morford et al., 2005, 2012; Tribovillard et al., 2006). The premise of this approach is that the strength of sedimentary carbon turnover, which is controlled by the flux of labile carbon to the sediments, strongly affects the vertical distribution of redox domains within sediments (oxic, suboxic, sulfidic), which in turn is reflected in solid-phase redox element distributions and fluxes (i.e., some elements are removed by dissolution and diffusion, others concentrated by precipitation) (Froelich et al., 1979; Calvert and Pedersen, 1993). Under suboxic and sulfidic conditions, other electron acceptors besides O_2 (such as NO_3^- , Mn(IV), or SO_4^{2-}) become important. Thus, sediment profiles of Mn and total and reduced sulphur can provide an indication of the vertical distribution of the redox domains (Thomson et al., 2001). Other redox elements such as Re, U, Cd, and Mo form insoluble species under reducing conditions in the sediments (i.e., authigenic accumulations). The presence or absence of Re, U, Cd, and Mo enrichments in sedimentary deposits has been interpreted as an indicator of reducing conditions and used as a proxy for reconstruction of paleoproductivity and paleoredox conditions in ancient oceans (Crusius and Thomson, 2000; Tribovillard et al., 2006). Quantitative utilization of redox-sensitive elements (i.e., statistical analysis of trends in authigenic accumulation rates) remains rare (cf., Böning et al., 2004; McManus

et al., 2006). However, variations in accumulation rates of authigenic Cd, Re, U, and Mo in continental margins with generally oxygenated waters, including the Laurentian Trough in the Gulf of St. Lawrence (Sundby et al., 2004), the Strait of Georgia (Macdonald et al., 2008), the Mid-Atlantic Bight, eastern United States (Morford et al., 2012) and Hudson Bay (Kuzyk et al., 2011), are consistent with variations in organic matter forcing (i.e., flux of labile carbon to the seafloor). The strength of sedimentary carbon turnover controls the rates of many important benthic processes such as denitrification and sedimentary iron reduction, with feedbacks to nutrient availability and rates of primary production in Arctic shelf systems (Esch et al., 2013; Horak et al., 2013). Additionally, sedimentary carbon turnover controls either directly or indirectly the extent to which Arctic sediments may represent a sink for trace metals (Macdonald and Gobeil, 2012). However, there may be multiple controls on sedimentary enrichments of trace metals, and multi-element sets of geochemical data provide opportunities to improve our fundamental understanding of modern oceanic and sedimentary geochemistry of these elements, and thereby improve their application as paleotracers.

Here, we analyze the distributions and accumulation rates of redox-sensitive elements (S, Mn, Mo, U, Cd, Re) in a set of 27 sediment cores collected along a section extending from the North Bering Sea to Davis Strait via the Canadian Archipelago (Fig. 1). Based on an understanding of the sedimentation rates and surface mixing in these cores (Kuzyk et al., 2013), and a characterization of the amounts and sources of organic carbon in surface sediments (Goñi et al., 2013), we use these data to (i) document the early diagenetic properties of Arctic margin sediments along the North American continent, (ii) evaluate labile organic supply as a controlling factor in the concentration profiles and accumulation rates of the studied elements; and (iii) compare the accumulation rates along this margin with rates reported for other oceans.

2. STUDY AREA

The key characteristics that define the NAAM sediments are average water depths, high degree of river (terrestrial organic matter) influence, large range in primary production, organic carbon rain rate, sediment accumulation rate, well-oxygenated bottom waters ($[O_2] > 200 \,\mu\text{mol L}^{-1}$) (Carmack et al., 2010), and widespread surface mixing by macrobenthos. Beginning at the margin's western extreme (Fig. 1), the North Bering and Chukchi Shelves are shallow, productive shelves, strongly influenced by nutrient-rich Pacific water that enters the Arctic Ocean through Bering Strait. Due to the import of nutrients, the Chukchi Shelf is one of the most productive areas in the world ocean; furthermore, due to shallow water depths, organic carbon production in the water column is tightly coupled to carbon deposition to the sediments (Grebmeier and Cooper, 1995; Grebmeier et al., 2006). The sediments in the North Bering and Chukchi Shelf regions support rich benthic communities (Dunton et al., 2005; Grebmeier et al., 2006) and are characterized by vigorous and deep biomixing (Esch et al., 2013; Kuzyk et al., 2013). Barrow Canyon cuts the shelf break at the eastern edge of the Chukchi Sea (Fig. 1) and is a site of upwelling events as well as dense (brine-rich) shelf water outflows (Pickart et al., 2005). Upper Barrow Canyon is a regional 'hotspot', with high productivity and high infaunal benthic biomass (Grebmeier et al., 2006), and deeper parts of the canyon are sites of enhanced particle and organic matter deposition (cf., Goñi et al., 2013; Kuzyk et al., 2013). Sediments in the Chukchi Sea and especially Barrow Canyon are also characterized by relatively high contributions of terrestrial organic matter, perhaps supplied by the Yukon River and/or coastal or subsea permafrost (McManus et al., 1969; Goñi et al., 2013). Moving eastward, the Beaufort Shelf (Fig. 1) comprises a narrow, sediment-starved shelf along the Alaskan north slope and a wider, Mackenzie River-dominated shelf further to the east (Macdonald

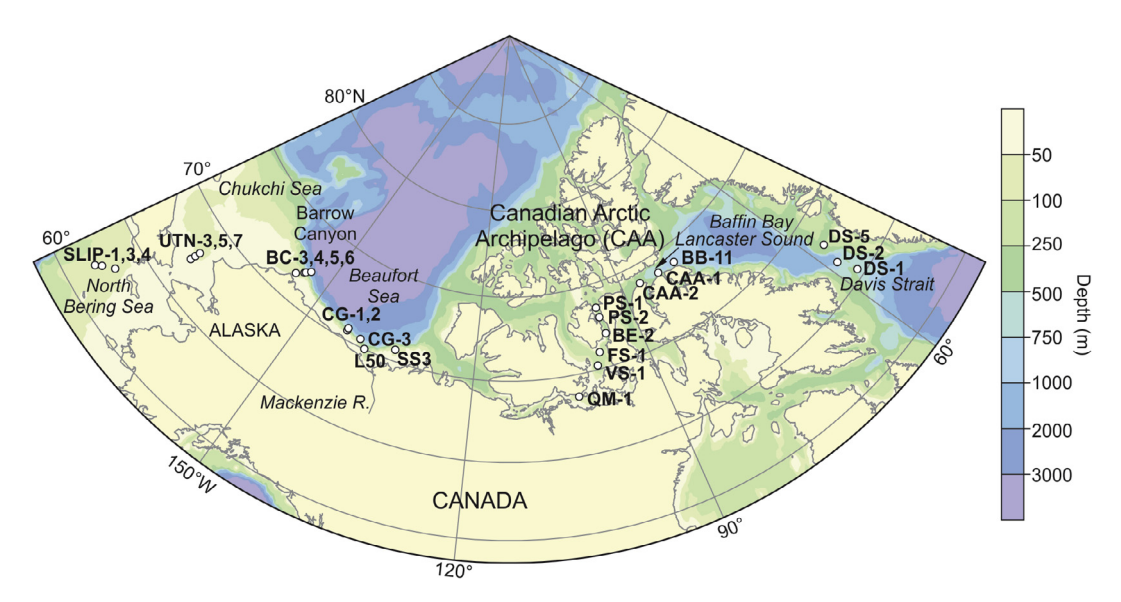


Fig. 1. Map of North American Arctic margin showing various subregions and approximate locations of 27 box cores examined in this study.

et al., 1998). This shelf is seasonally covered by landfast ice out to approximately the 20 m isobath, beyond which is the flaw lead and freely-drifting polar pack ice. The Beaufort Shelf is oligotrophic, supporting primary production levels on the order of $30-70 \text{ gC m}^{-2} \text{ yr}^{-1}$ (Sakshaug, 2004; Carmack et al., 2006). Several local rivers (Kuparuk, Colville, Sagavanirktok) discharge along the Alaskan coast but the Mackenzie River dominates the Beaufort Shelf in terms of sediment ($\sim 127 \times 10^6 \text{ tons yr}^{-1}$) and particulate organic carbon ($\sim 1.8 \times 10^9 \,\mathrm{kg} \,\mathrm{yr}^{-1}$) supply (Goñi et al., 2000). Ancient material, which may include old pre-aged soil material as well as fossil bitumen or kerogen, is believed to contribute about 60-70% of this terrestrial organic carbon; this material is believed to be partly remineralized (up to 25%) and partly deposited in outer shelf sediments (Goñi et al., 2005, 2013). Farther eastward is a complex shelf consisting of a network of channels known as the Canadian Archipelago (Fig. 1). Through these channels, there is a net (eastward) outflow of water from the Arctic Ocean to Baffin Bay and eventually the North Atlantic. The Archipelago is covered by landfast ice during most of the year. It receives widely distributed runoff from a myriad of small rivers and has generally very low primary production (20-40 gC m⁻² yr⁻¹), with higher values occurring in localized areas of strong flow and tidal mixing (Sakshaug, 2004; Carmack et al., 2006). Lancaster Sound lies at the eastern limit of the Canadian Archipelago and is one of the three main channels connecting the Archipelago to Baffin Bay and Davis Strait (Fig. 1). Arctic waters then flow southward along the west side of Baffin Bay, while on the east side of Baffin Bay, the West Greenland Current transports Arctic outflow via Fram Strait northward, together with Irminger Sea water (Cuny et al., 2005). Primary production averages 150 gC m⁻² yr⁻¹ in the productive Northwater Polynya, which is located in northern Baffin Bay, and 60-120 gC m⁻² yr⁻¹ throughout the remainder of the bay and Davis Strait (Sakshaug, 2004; Carmack et al., 2006).

3. METHODS

3.1. Sampling and analysis

The majority of the sediment cores analyzed in this study were collected during oceanographic missions aboard the Canadian Coast Guard Ships Wilfrid Laurier in July 2007 and Louis S. St. Laurent in July 2008. The 25 core sites visited during these two successive years span water depths of 50–2125 m (Table 1) and are distributed widely along the North American Arctic and Subarctic coastline from the North Bering Shelf in the west to Davis Strait in the east (Fig. 1). The North Bering Shelf (stations SLIP-1,3,4), Chukchi Shelf (stations UTN-3,5,7), Barrow Canyon area in the northeast Chukchi Shelf (stations BC-3,4,5,6), and Beaufort Sea slope (stations CG-1,2,3) were sampled in 2007 and the Canadian Arctic Archipelago (stations QM1, VS1, FS1, BE2, PS2, PS1), Lancaster Sound (stations CAA2, CAA1, BB11), and Davis Strait (stations DS-1, 2,5) were sampled in 2008. Also included in this study are two cores (L50 and SS3) collected in 1990 from the eastern portion of the Beaufort Shelf (i.e., Mackenzie Shelf) at water

depths of 711 m and 274 m, respectively (see Gobeil et al., 1991 for details).

The sediment cores were collected using a box-corer, which penetrates the seafloor to a maximum of 50 cm and has a collection area of 600 cm². The cores were subsectioned horizontally aboard the ship, generally into 0.5 cm intervals for the top 2 cm, 1 cm intervals for the 2–10 cm depth interval, and 2, 3 or 5 cm intervals for the remainder of the core. Sediment from the outermost 3–5 cm of the box was discarded. Sediment samples were placed in plastic bags or bottles and kept frozen for later chemical analysis.

Subsamples for elemental (Ca, Al, S, Mn, Cd, Mo, U, and Re) analyses were freeze-dried, homogenized by grinding and totally digested with a mixture of HNO₃, HClO₄ and HF as described in Kuzyk et al. (2011). The solutions were analyzed for Ca, Al, S and Mn by ICP-AES (Inductively Coupled Plasma-Atomic Emission Spectroscopy) and for Cd, Mo, U and Re by ICP-MS (Inductively Coupled Plasma-Mass Spectroscopy) using external calibrations. Calcium extracted from the sediments with an HCl solution (1 N) at room temperature during 12 h was also determined by ICP-AES. Hereafter, we assume that Ca released by this chemical treatment represents essentially that associated with carbonate minerals. The precision and accuracy of the lab analyses were assessed over the long term by replicate analyses of the standard reference sediments PACS-2 and MESS-3. Good agreement was obtained between certified and measured values (Table 2). All concentration data are reported on a dry-sediment basis after correcting for salt content. Furthermore, total S (S_{tot}) was adjusted by subtracting porewater S, which was estimated using measured porosity values, assuming that the porewater S concentration is identical to seawater SO_4^2 concentration (28 mM). Such an assumption is justified by the expected low SO_4^{2-} reduction rate for most of the cores and the relatively constant porewater SO₄²⁻ concentration with sediment depth in cores L50 and SS3 (28.6 \pm 0.44 mM, n = 39; Gobeil et al., 1991).

Three operationally-defined reduced inorganic sulphur fractions, i.e., acid-volatile sulphide (AVS), chromiumreducible sulphur (CRS) and elemental sulphur (ES), were determined in selected sediment subsamples. The method used is based on the work of Canfield et al. (1986) and Hsieh and co-workers (Hsieh and Yang, 1989; Hsieh et al., 2002). About 0.5 g of wet sediment was weighed and placed in a Teflon reactor with 50 mL demineralised deoxygenated water containing 100 µL of 1 N NaOH. AVS (≈amorphous FeS, +mackinawite + poorly crystallized greigite) was first extracted by the addition of 1 mL ascorbic acid and 10 mL 6 N HCl. The released sulphide was entrained by an O₂-free nitrogen stream, trapped in a NaOH solution and subsequently measured by the blue methylene colorimetric method (Cline, 1969). To release S associated with pyrite, the residue from the first lixiviation was then leached with 7.5 mL of an acidic Cr(II) solution, prepared by dissolving CrCl₃·6H₂O in presence of HCl and passing this solution trough a column of Zn amalgamated to Hg to reduce Cr(III) to Cr(II). Lastly, to release ES the residue from the previous treatment was leached

Table 1
Location and characteristics of sediment cores.

Region and core	Water depth	Sediment porosity	Organic carbon (%)	Surface mixed	Sediment accumulation rate
number	(m)	(Mean (SD))	(Mean (SD))	layer (cm) ^a	$(g cm^{-2} yr^{-1})^a$
North Bering Sea Si	helf				
SLIP1	80	0.67 (0.07)	1.06 (0.19)	4	0.39 (0.19-1.2)
SLIP3	73	0.67 (0.09)	1.06 (0.27)	4	0.33 (0.14–2.2)
SLIP4	73	0.77 (0.06)	1.75 (0.21)	2	0.24 (0.15–0.34)
Chukchi Sea Shelf					
UTN3	50	0.62 (0.06)	0.97 (0.18)	>10	n/a, assumed 0.28 ^b
UTN5	51	0.65 (0.06)	1.25 (0.23)	5	0.28 (0.15-0.68)
UTN7	58	0.76 (0.05)	1.96 (0.33)	>5	n/a, assumed 0.28 ^b
Barrow Canyon					
BC3	186	0.84 (0.14)	4.50 (2.06)	>19	n/a, assumed 0.16 ^b
BC4	599	0.67 (0.07)	1.44 (0.22)	4	0.16 (0.12–0.24)
BC5	1015	0.64 (0.07)	1.36 (0.24)	2	0.05 (0.04-0.13)
BC6	2125	0.77 (0.04)	1.69 (0.11)	~7 °	~ 0.08
Beaufort Shelf					
CG1	204	0.66 (0.04)	1.07 (0.09)	2	0.18 (0.13-0.23)
CG2	619	0.78 (0.04)	1.20 (0.30)	1	0.07 (0.06–0.08)
CG3	566	0.77 (0.03)	1.36 (0.11)	2	0.07 (0.03-0.12)
L50	711	0.80 (0.05)		1	0.06 (0.05–0.09)
SS3	274	0.76 (0.05)		1	0.04 (0.04–0.05)
Canadian Archipelas	go				
QM1	113	0.76 (0.01)	0.86 (0.08)	1	0.11 (0.09-0.17)
VS1	210	0.71 (0.04)	0.70 (0.12)	1	≤0.04 (0.03–0.05)
FS1	141	0.61 (0.07)	0.72 (0.23)	2	≤0.09 (0.05–0.22)
PS1	245	0.68 (0.05)	0.77 (0.17)	1	0.06 (0.04-0.10)
PS2	340	0.63 (0.02)	0.43 (0.06)	1	≤0.21 (0.09–0.47)
BE2	431	0.67 (0.02)	0.89 (0.16)	1	0.11 (0.06–0.11)
Lancaster Sound					
CAA2	368	0.56 (0.02)	0.79 (0.04)	1	≤0.13 (0.09–0.20)
CAA1	630	0.70 (0.06)	1.61 (0.29)	4	0.18 (0.05–0.36)
BB11	850	0.81 (0.05)	1.78 (0.11)	1	0.05 (0.03–0.07)
Davis Strait					
DS2	780	0.58 (0.10)	0.47 (0.13)	0	≤0.063 (0.05–0.07)
DS1	575	0.53 (0.08)	0.43 (0.23)	2	0.075 (0.056–0.11)
DS5	340	0.43 (0.05)	0.29 (0.10)	2	0.10 (0.07-0.13)

^a Data from Kuzyk et al. (2013) with the exception of cores SS3 and L50 (Gobeil et al., 1991).

with 10 mL of dimethylformamide (DMF) in the presence of 2.5 mL of the Cr(II) solution and 2.5 mL of concentrated HCl (Hsieh and Yang, 1989). The evolved H₂S was trapped after each extraction in fresh NaOH solutions and determined colorimetrically. Precision of the measurements was evaluated from duplicate analysis of nine different samples with AVS, CRS and ES concentrations ranging from 0.2 to 198 μ g g⁻¹, 16 to 646 μ g g⁻¹ and 4 to 162 μ g g⁻¹, respectively. Coefficients of variation averaged 15%, 12%, and 23%. Here, we report total inorganic reduced sulphur species (S_{red}), calculated as the sum of the concentrations of AVS + CRS + ES.

Total carbon (TC) content was determined by high temperature combustion of samples using a NC2500 Thermo-Quest Elemental Analyzer (Goñi et al., 2013). Organic carbon (OC) contents were determined on splits of each

sample that were exposed to concentrated HCl fumes and 10% aqueous HCl prior to analysis to remove inorganic carbon. These treatments were done on pre-weighed samples in silver boats, which, after oven-drying, were wrapped in tin boats and analyzed by high temperature combustion using the same elemental analyzer. Inorganic carbon (IC) contents were determined as the difference between TC and OC. Replicate analyses of selected samples yielded analytical variability of less than 4% of the measured values.

3.2. Estimates of elemental lithogenic and authigenic concentrations

Lithogenic concentrations of the elements need to be accounted for before the distributions of authigenic phases of the redox-sensitive elements can be discussed. Here, we

^b These cores were deeply biomixed, thus sedimentation rates were not calculated from the data. For calculating accumulation rates, we have applied the sedimentation rates from nearby cores.

^c The 'surface' of core BC6 appears to have been buried recently beneath 7 cm of rapidly emplaced material and thus the sediment accumulation rate was estimated from the portion of the ²¹⁰Pb profile between 7 and 20 cm depth.

Table 2 Summary of precision and accuracy for major and trace element analyses.

	Certified value	Average \pm SD	N
PACS-2			
Al	$6.62\% \pm 0.32\%$	$6.34\% \pm 0.28\%$	51
Ca	$1.96\% \pm 0.18\%$	$1.92\% \pm 0.10\%$	51
Mn	$440 \pm 19~\mu g~g^{-1}$	$437 \pm 24~\mu g~g^{-1}$	51
S	$1.29\% \pm 0.13\%$	$1.24\% \pm 0.06\%$	51
Cd	$2.11 \pm 0.15~\mu g~g^{-1}$	$2.27\pm0.16~\mu g~g^{-1}$	16
Mo	$5.43 \pm 0.28~\mu g~g^{-1}$	$5.15 \pm 0.62~\mu g~g^{-1}$	16
Re	n/a	$7.37 \pm 0.30 \ \mathrm{ng} \ \mathrm{g}^{-1}$	13
U	$3 \mu g g^{-1*}$	$2.25 \pm 0.29~\mu g~g^{-1}$	15
MESS-3			
Al	$8.59\% \pm 0.23\%$	$8.30\% \pm 0.51\%$	53
Ca	$1.47\% \pm 0.06\%$	$1.40\% \pm 0.07\%$	53
Mn	$324 \pm 12~\mu g~g^{-1}$	$319 \pm 15~\mu g~g^{-1}$	53
S	0.19%*	$0.18\% \pm 0.01\%$	53
Cd	$0.24 \pm 0.01~\mu g~g^{-1}$	$0.28 \pm 0.05~\mu g~g^{-1}$	11
Mo	$2.78 \pm 0.07~\mu g~g^{-1}$	$2.69 \pm 0.24~\mu g~g^{-1}$	11
Re	n/a	$6.12 \pm 0.51 \; \mathrm{ng} \; \mathrm{g}^{-1}$	12
U	$4 \mu g g^{-1*}$	$3.55 \pm 0.62~\mu g~g^{-1}$	12

^{*} Information value only.

assume that the lithogenic contribution to S, Mo, and Cd in the sediment samples may be estimated from the Al content: $E_{\text{litho}} = \text{Al}_{\text{tot}} \times (E/\text{Al})_{\text{ref}}$, where E_{litho} is the lithogenic concentration of element E, Altot is the total measured Al content and $(E/Al)_{ref}$ is the best estimate for the E/Al ratio characterizing the lithogenic component of the sediments at the sampling site. Specifically, we used the S/Al ratio $(0.76 \times 10^{-2} \text{ g g}^{-1})$ and the Mo/Al ratio $(11 \times 10^{-6} \text{ g g}^{-1})$ provided by Rudnick and Gao (2003) as (S/Al)_{ref} and (Mo/Al)_{ref}, respectively. The former ratio reflects upper continental crust and the latter ratio lies within the range of values for igneous rocks and sandstones $(6-19 \times 10^{-6}$ $g g^{-1}$, Turekian and Wedepohl, 1961) and is consistent with the more recently reported value in the revised edition of Rudnick and Gao (2003). For Mn, we followed Macdonald and Gobeil (2012) and applied the Mn/Al ratio for Chukchi Shelf sediments $(5.9 \times 10^{-3} \text{ g/g})$ to North Bering-Chukchi and Barrow Canyon and the Mn/Al ratio for Beaufort sediments $(3.3 \times 10^{-3} \text{ g/g})$ to the Beaufort and all areas further east. Concentrations of authigenic Cd were calculated using a background Cd/Al ratio 1.5×10^{-6} g/g (Borchers et al., 2005). In most cores, including those from the Canadian Archipelago (BE2, PS1 and PS2) and Lancaster Sound (CAA2), which had a high content of non-biogenic carbonate (Goñi et al., 2013), the calculated background concentrations are close to the minimum measured concentrations of Mo, Mn, and Cd, thus suggesting that carbonate particulates contribute negligibly to these elements in the sediments.

In contrast, the contribution of U from non-biogenic carbonate could not be neglected. For U, therefore, we assumed that $U_{litho} = [Al_{tot} \times (U/Al)_{ref}] + [Ca_{HCl} \times (U/Ca)_{ref}]$, where $(U/Al)_{ref}$ is $18 \times 10^{-6} \, g \, g^{-1}$ (Taylor and McLennan, 1986) except for the Mackenzie Shelf samples where we used the higher $(U/Al)_{ref}$ value reported previously for this region $(35 \times 10^{-6} \, g \, g^{-1})$ (Vigier et al.,

2001); Ca_{HCl} is the measured concentration of HCl-extractable Ca in the sediments; and $(U/Ca)_{ref}$ is 7.3×10^{-6} g g⁻¹, a value characterizing non-biogenic carbonate (Turekian and Wedepohl, 1961).

Lastly, considering that the crustal abundance of Re is not yet well constrained (Helz and Adelson, 2013), we have arbitrarily assumed that Re_{litho} is equivalent to the average measured concentration of Re in our sediment samples (n=81) from the Canadian Archipelago having Re concentration values lower than 1 ng g^{-1} . This background $(0.65 \text{ ng g}^{-1}, \text{ s.d.} = \pm 0.16)$ is consistent with recent published assessments $(0.2-0.6 \text{ ng g}^{-1}; \text{ Peucker-Ehrenbrink}$ and Jahn, 2001; McLennan, 2001; Helz and Adelson, 2013).

Hereafter, the authigenic concentration of element E (E_A) is obtained by subtracting $E_{\rm litho}$ from the total concentration ($E_{\rm tot}$) and its inventory in a specific segment of the core is provided by the sum of $E_A \times (1-\phi) \times \Delta l \times \rho$ for each individual sediment layer composing that segment, where ϕ and Δl are respectively the sediment porosity and thickness of each layer, and ρ is the solid-phase density assumed to be 2.65.

4. RESULTS

The vertical profiles of measured elements (OC, S_{tot}, Mn, Mo, Cd, U and Re) and authigenic phases of the redox-sensitive elements (S_A, Mn_A, Mo_A, Cd_A, U_A and Re_A) in the sediments are illustrated in Fig. 2a for Bering and Chukchi Shelves, 2b for Barrow Canyon and Beaufort Shelf, 2c for Canadian Archipelago and 2d for Lancaster Sound and Davis Strait. The vertical profiles of S_{red} in the sediments are illustrated in Fig. 3. Raw data are provided in Appendix 1.

The OC content in the sediment cores across all regions is highest at the surface, decreases within the top few cm, and then remains roughly constant throughout deeper portions of the cores. The OC values in deep sections of the cores range from very low values (0.1–0.6%) in cores from Davis Strait (Fig. 2d) and the Canadian Archipelago (Fig. 2c) to very high values (~4.7%) at the head of Barrow Canyon (core BC3; Fig. 2b). The wide range of average OC content in the cores (Table 1) implies strong variation from site to site in organic matter supply and/or preservation (see also Goñi et al., 2013).

The concentration of Stot in many cores, such as in Chukchi and Bering Shelves and in Barrow Canyon, increases from the top to the bottom (Fig. 2a and b). At our sampling sites from these regions, S_{tot} often reaches values higher than 4 mg g⁻¹ at depth in the cores, while S_{red} reaches values of 2– 4 mg g⁻¹ (Fig. 3). S_{red} thus accounted for >50% of the S_{tot} at depth in these cores. In contrast, in other regions of the NAAM, Stot first decreases below the sediment-water interface but then increases slightly downward, reaching again maximum values at the bottom of the cores. This pattern is observed in the three cores from Lancaster Sound (Fig. 2c), and in two cores from the Beaufort Shelf (CG1 and CG2; Fig. 2b) and two cores from Davis Strait (DS1 and DS5; Fig. 2d). In these locations, where maximum values of Stot do not exceed about $1-2~{\rm mg~g^{-1}}$, $S_{\rm red}$ reaches maximum values of 0.2–1.2 mg g⁻¹ (Fig. 3) and again accounts for a major

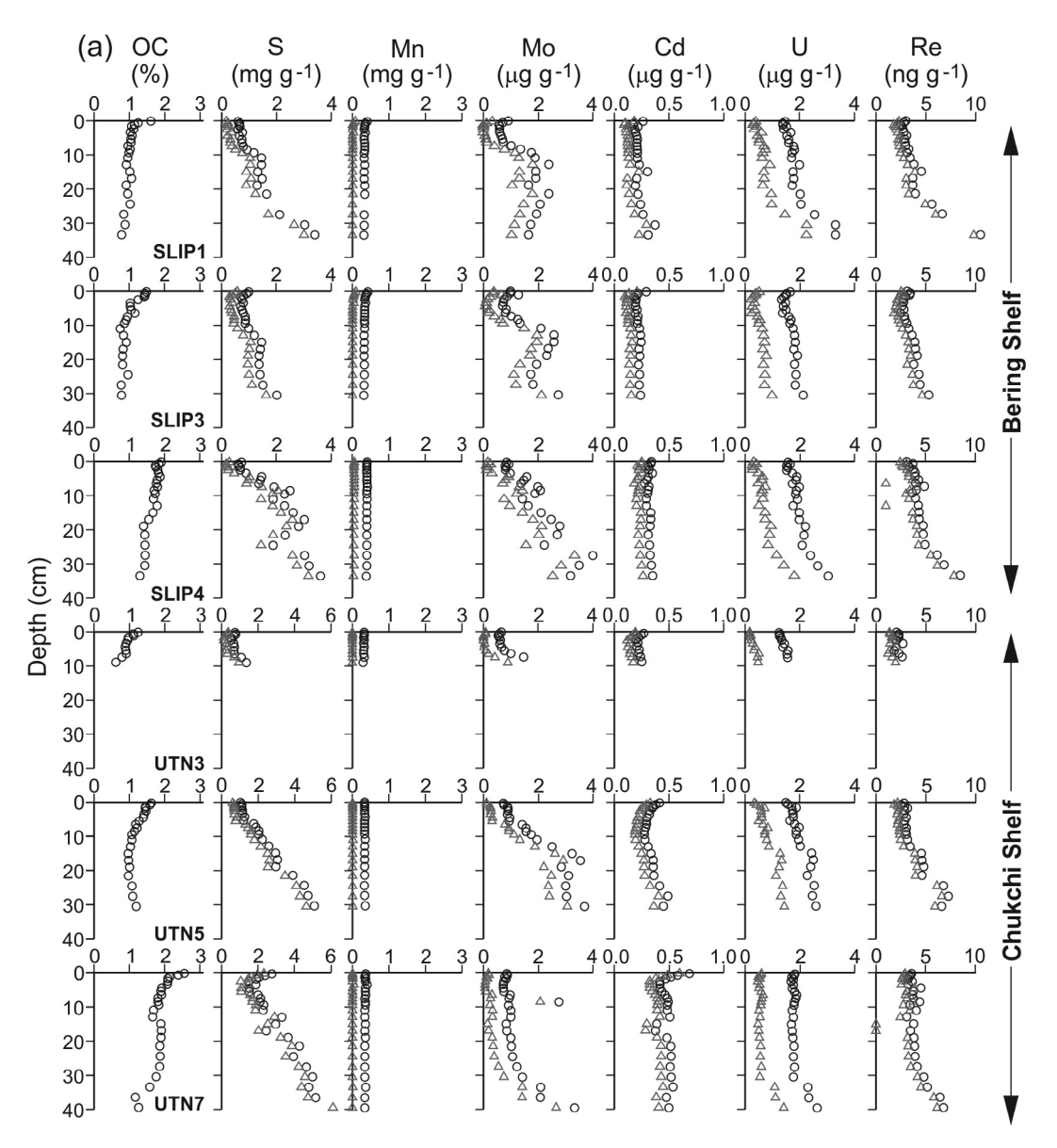


Fig. 2. Profiles of measured elements (OC, Mn, S, Mo, Cd, U, and Re) (circles) and estimated concentrations of authigenic phases (triangles) in cores from the Bering–Chukchi shelves (a), Barrow Canyon and the Beaufort Shelf (b), the Canadian Archipelago (c), and Lancaster Sound and Davis Strait (d).

fraction of S_{tot} at depth in the cores. Finally, S_{tot} and S_{red} are both low ($S_{tot} < 0.1 \ mg \ g^{-1}$) and do not vary much with depth at all sampling sites from the Canadian Archipelago (Fig. 2c) and at specific sites from the Beaufort Shelf (CG3, L50 and SS3; Fig. 2b) and Davis Strait (DS2; Fig. 2d).

The vertical distribution of Mn in the sediments also strongly varies with location in the NAAM. In sediments having elevated S inventories, including Bering-Chukchi shelves and specific cores from Barrow Canyon, Lancaster Sound and Davis Strait, Mn concentrations are low (<0.5 mg g⁻¹) throughout the cores although a weak surface enrichment may be observed in some cores. This 'flat' vertical profile is in sharp contrast with all other cores that have Mn elevated in a surface layer, then decreasing to low and relatively constant concentrations at depth. This general pattern is typical but there are important regional dif-

ferences in the thickness of the surface layer enriched in Mn as well as in the level of enrichment. In some cores from the Canadian Archipelago (PS2 and BE3; Fig. 2c) and the Beaufort Shelf (CG2 and CG3; Fig. 2b), where the S contents of the sediments are the lowest, the Mn enriched surface layer is more than 10 cm thick and the maximum values of the Mn concentrations within the enriched layer reach 10-20 mg g⁻¹. In cores having a substantive Mn inventory, the full profiles of Mo remarkably parallel those of Mn. The covariation between Mo and Mn is also observed near the sediment-water interface in the cores having a thin enriched Mn layer (CG1 and VS1; Fig. 2b and c). In contrast, beneath the Mn-rich layer, where Mn concentrations become consistently low, both Mo and S progressively increase with depth. Molybdenum and S (Stot and Sred) covary at sampling sites where the Mn

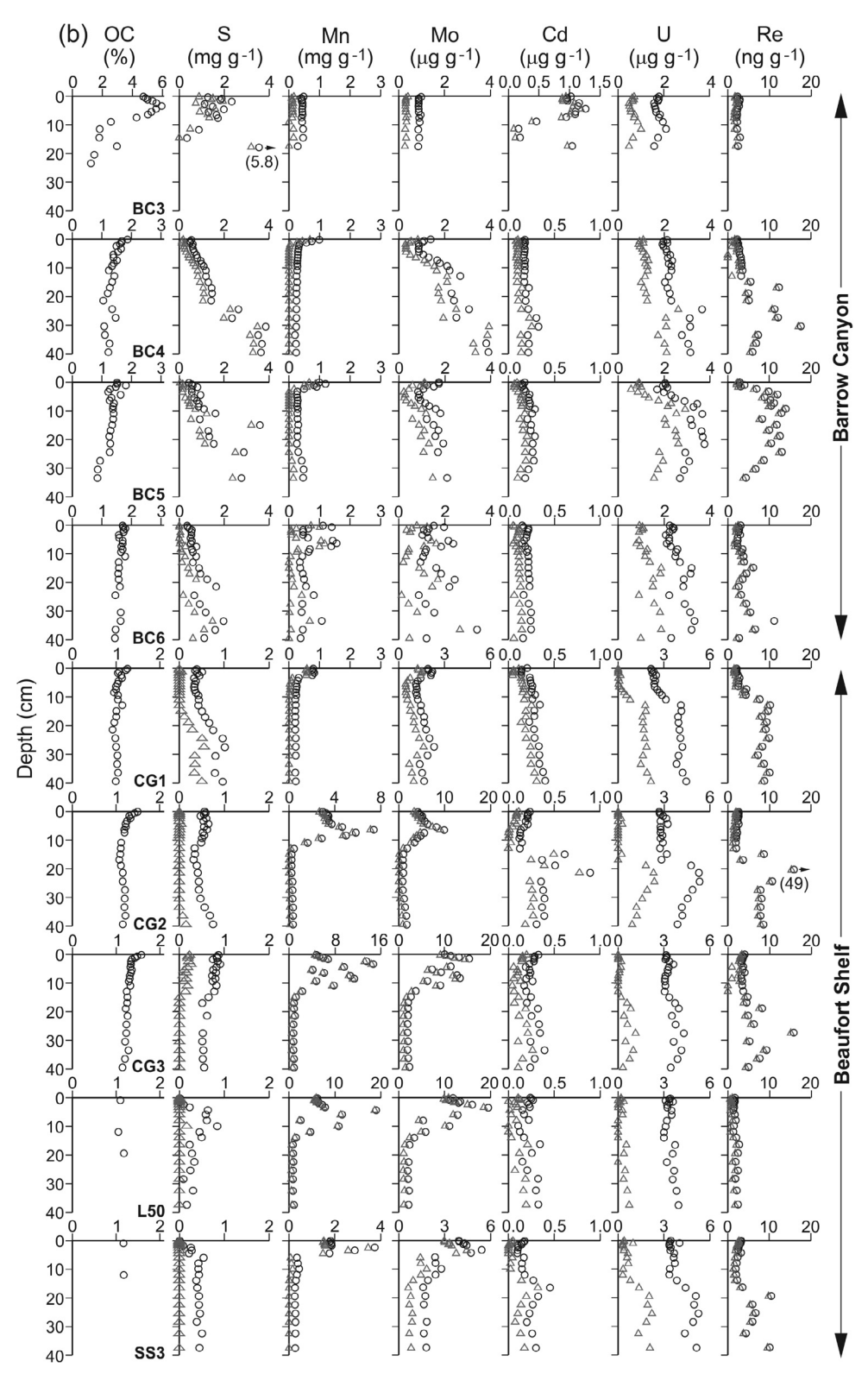


Fig 2. (continued)

concentrations and inventories in the sediments are the lowest (Bering–Chukchi shelves and Barrow Canyon). At many of these sites, Mo increases progressively from $\sim\!\!1~\mu g~g^{-1}$ in surface sediments to $4~\mu g~g^{-1}$ at 30–40 cm depth.

The profiles of Cd, U and Re exhibit, contrary to Mo, no clear similarity with any portions of the Mn profiles. With few exceptions, the overall trend in the profiles of these three elements is an increase with depth. In most

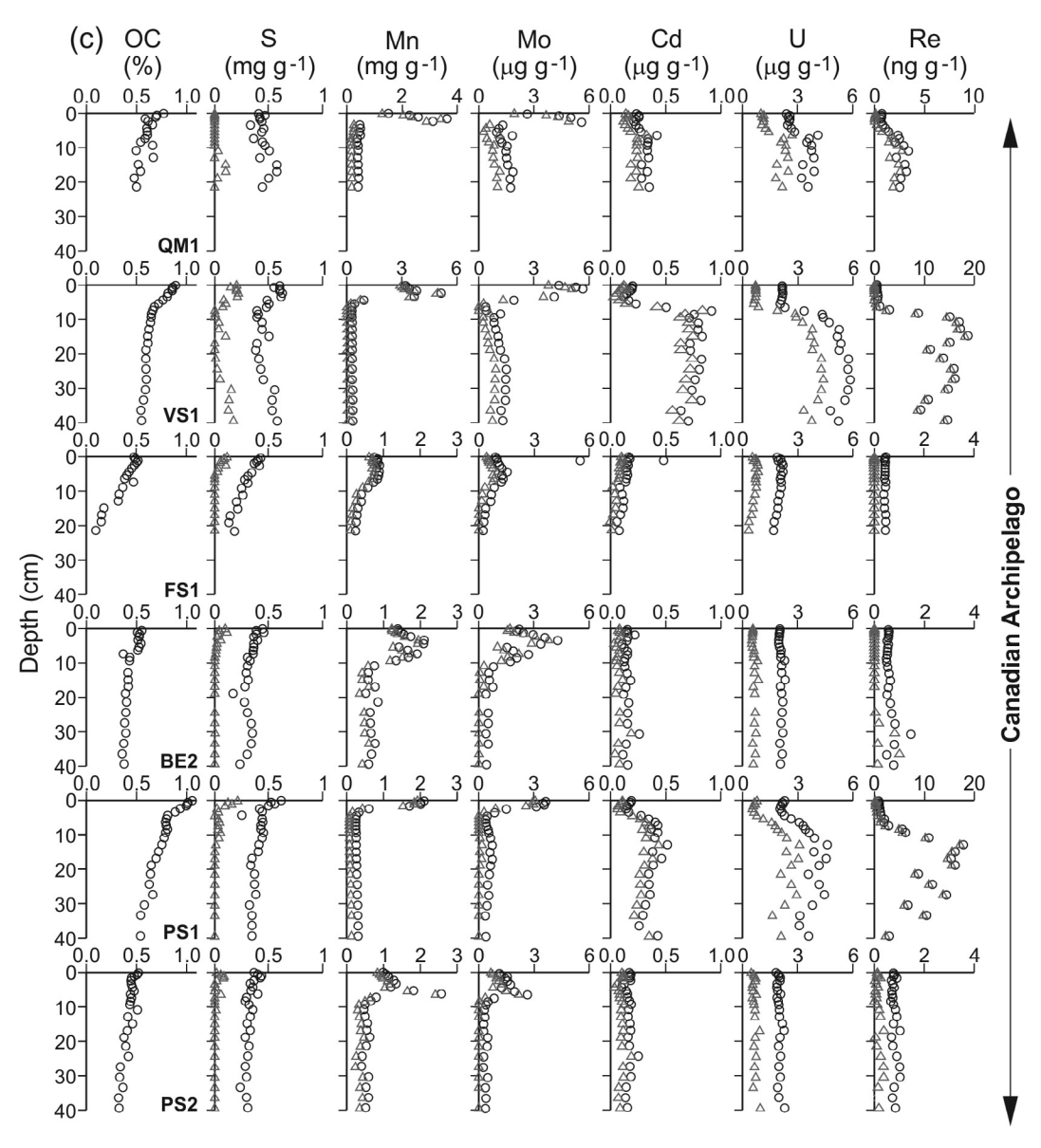


Fig 2. (continued)

cores, concentrations increase abruptly and then remain constant with depth; in a few cores (e.g., CG2), concentrations increase and then slightly decrease with depth. For the Bering and Chukchi Shelves (Fig. 2a), the concentrations of U, Re and, to a lesser extent, Cd tend to increase with depth throughout the cores similar to $S_{\rm tot}$ and $S_{\rm red}$. In the cores having a surface enriched Mn layer, the concentration increases occur close to the base of the Mn layer, approximately where $S_{\rm red}$ begins to increase significantly.

5. DISCUSSION

5.1. Regional patterns in sedimentary organic carbon oxidation as reflected by Mn and \boldsymbol{S}

Microbial OC metabolism at the seafloor consumes O₂, thus establishing a concentration gradient in which O₂ decreases with depth in the sediments and progressively changes the redox environment. Depending on water column productivity and OC deposition at the ocean bottom, the thickness of the aerobic layer in the sediments may be a few mm or less in shallow productive waters, while it may extend to several cm in poorly productive marine regions (cf., Canfield, 1993; Cai and Sayles, 1996; Thomson et al., 2001). Due to the upward diffusion of Mn(II) into the oxic surface layer, where it oxidizes, that aerobic layer is often found enriched in Mn oxyhydroxides, the thickness of which can be used as an indicator of organic matter metabolism. From the considerable variation in the thickness of surface Mn-rich layers in the NAAM sediments (Fig. 2), we thus infer significant differences in the average (maximum) O₂ penetration depth in the sediments and intensity of aerobic OC metabolism. The thickness of the Mn-enriched layer is organized regionally: undetectable or very thin lay-

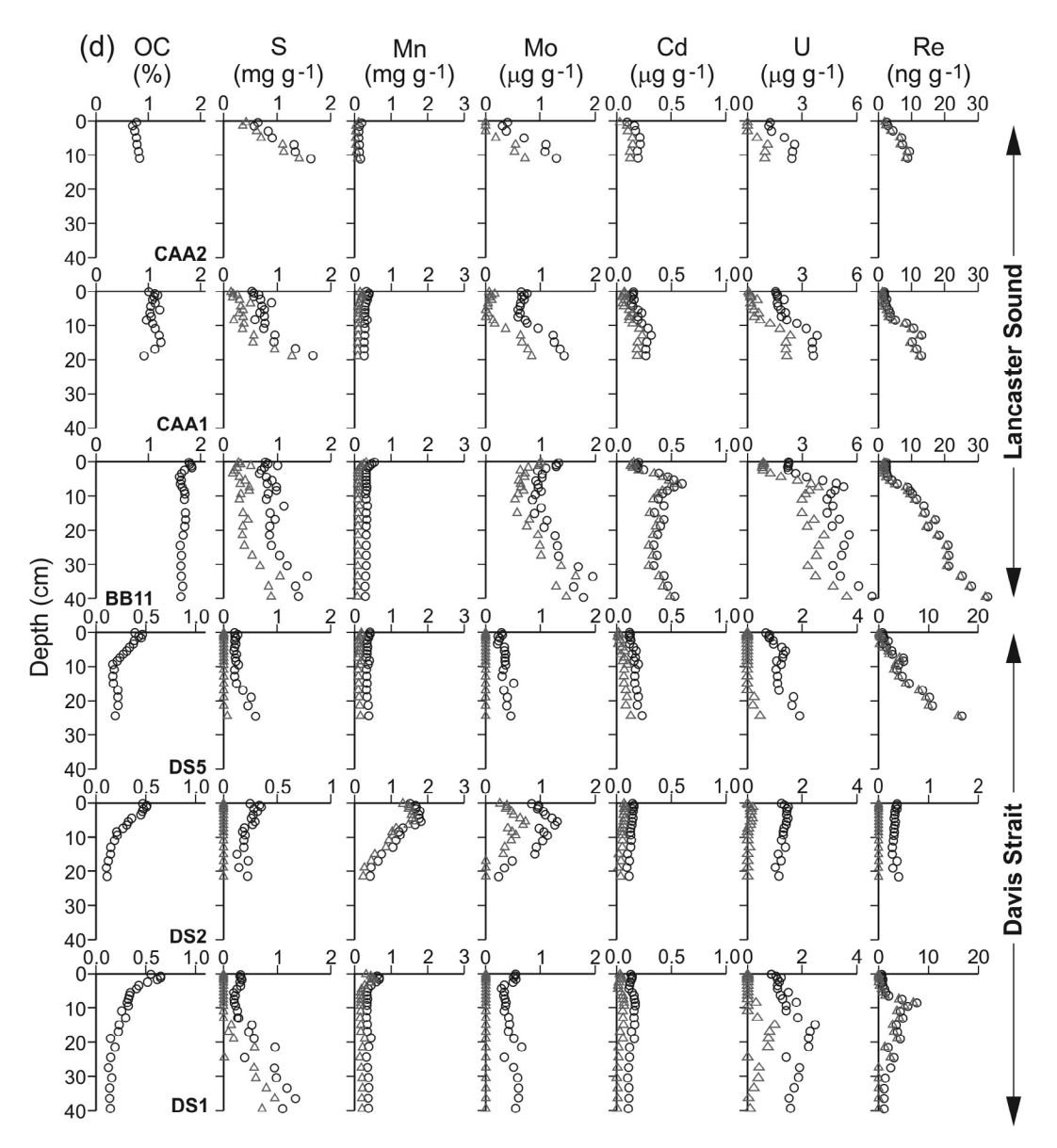


Fig 2. (continued)

ers (<0.5 cm) of surface Mn enrichment imply strong OC flux and metabolism in the Bering–Chukchi shelves, thin layers (1–5 cm) of surface Mn enrichment imply lower aerobic OC metabolism in Barrow Canyon and Lancaster Sound, and thick layers (5–20 cm) of surface Mn enrichment imply deep $\rm O_2$ penetration and much lower OC metabolism in the Beaufort Shelf, Canadian Archipelago, and Davis Strait.

Although the large-scale distribution of Mn-rich surface layers in sediments along the NAAM may generally reflect the spatial patterns in carbon respiration, caution is required in interpreting redox parameters like Mn because the O₂ penetration depth and consequently changes in surface Mn distribution can undergo rapid and dramatic excursions in response to variations in labile OC flux (cf., Fig. 3 in Katsev et al., 2006). Theoretically, steady-state diagenesis in sediments would generate a single Mn peak

in a narrow depth interval close to the depth of O₂ penetration assuming the surface mixed layer (SML) is thin relative to the aerobic layer. If this assumption is not true, the Mn enrichment would become more evenly distributed throughout the SML (Thomson et al., 2001; Katsev et al., 2006). In our data set, many of the Mn profiles have narrow peaks (see, for example, CG2, QM1, VS1 in Fig. 2b and c), which indicate SML depths (Table 1) less than the Mnenriched depth, whereas cores from the Bering-Chukchi shelves and Barrow Canyon have no evident Mn peaks. There are only a few cores (e.g., CG3 and BE2) that have multiple peaks in their Mn profiles, which imply fluctuations of the redox boundaries (i.e., non-steady state diagensis in which there has been partial Mn oxyhydroxide reduction followed by a return to oxic conditions such that the Mn-rich layer is thinned; Katsev et al., 2006). However, seasonal and interannual variations in OC flux that can

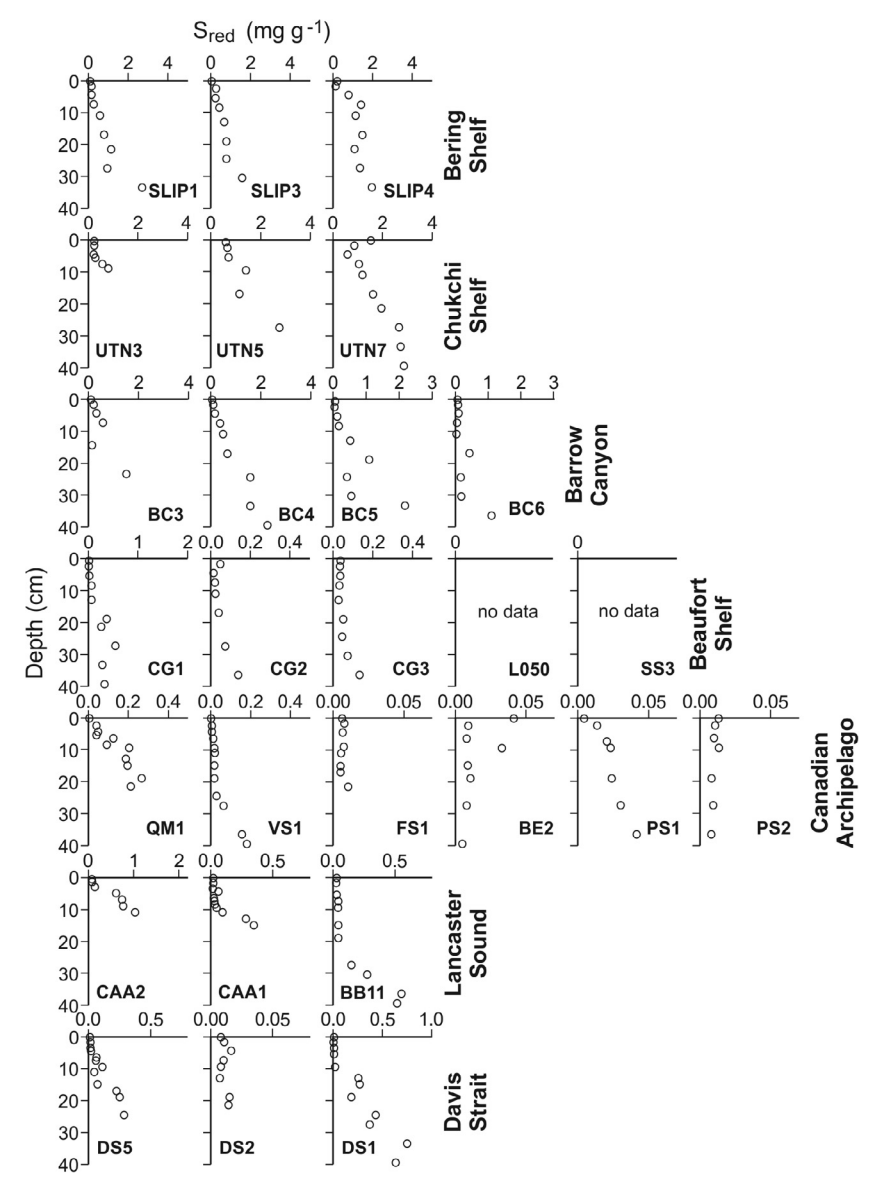


Fig. 3. Profiles of total reduced sulphur $(S_{red} = AVS + CRS + ES)$ in the cores.

bring about fluctuations of redox boundaries are probably the norm along the NAAM. Thus, the thickness of the surface Mn-rich layers in sediment cores can only be used qualitatively to compare reduction intensity among the areas. This limitation provides part of the rationale for examining other redox-sensitive elements that form authigenic phases in the sediments.

The progressive increases of S_{tot} and S_{red} from the sediment surface to the bottom of the cores in which the enriched Mn layer is absent or very thin, or from the base of the Mn layer to the bottom in those cores with a substantial Mn-enriched layer (Fig. 2), imply formation and burial in the sediments of authigenic sulphide phases. These phases consist mainly of pyrite, Fe monosulphide and other amorphous metal sulphides that have formed as a consequence of anaerobic respiration using sulphate as terminal electron acceptor. Similar to Mn, the distributions of S_{red}

and Stot (Fig. 2) across the NAAM are also organized regionally. Inventories of authigenic S (S_A) below the Mn-rich layer, for example, decrease from an average of 60 mg cm⁻² in the Bering-Chukchi shelf and Barrow Canyon sediments to \sim 12 mg cm⁻² in Lancaster Sound sediments and <2 mg cm⁻² in the Beaufort Shelf, Canadian Archipelago and most Davis Strait sediments (Fig. 4). There is an apparent absence of reduced S accumulation in cores FS1, BE2, and PS2 from the Canadian Archipelago and DS2 from Davis Strait, which indicates minimal anaerobic OC oxidation coupled to sulphate reduction. Previous workers have suggested that Mn(IV) and Fe(III) are the dominant terminal electron acceptors for OC metabolism in most Arctic Ocean margin sediments, with the exception of highly productive areas where sulphate becomes the dominant oxidant (Kostka et al., 1999; Vandieken et al., 2006; Nickel et al., 2008). Our results seem therefore consis-

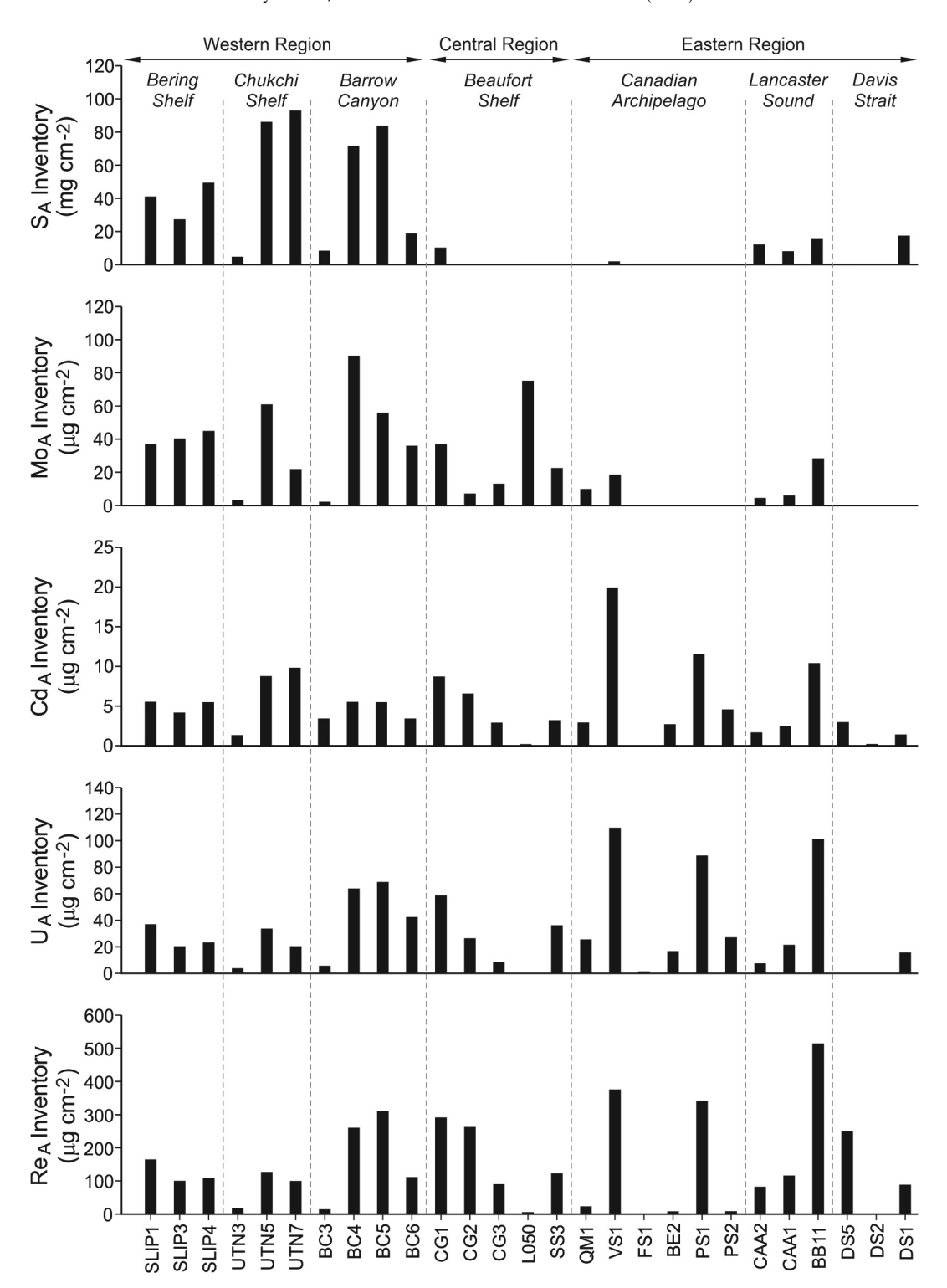


Fig. 4. Inventories of the authigenic component of the elements (S, Mo, Cd, U and Re) in reducing sediments, i.e., below the Mn-rich surface layers, across the seven subregions of the North American Arctic margin.

tent with previous studies; they indicate a greater importance of sulphate reduction in the Bering-Chukchi shelves and Barrow Canyon, where both S_{tot} and S_{red} concentrations reach maximum values at the bottom of the cores (Fig. 2a and b), and only a minor role for sulphate reduc-

tion in the Canadian Archipelago, Davis Strait and Beaufort Shelf regions, where these concentrations are much lower. This finding of much stronger reducing conditions in the Bering-Chukchi shelf is consistent with porewater O₂ micro-profiles in a separate study (Esch et al., 2013)

and explains the absence of a Mn-rich surface layer in these sediments (Fig. 2a). Overall, the sediment profiles of Mn, S_{tot} (Fig. 2) and S_{red} (Fig. 3) and the sediment inventories of authigenic S (Fig. 4) indicate clear regional domains in OC deposition and metabolism in the sediments: (i) strong reducing conditions in the Bering–Chukchi shelves and Barrow Canyon; (ii) moderate reducing conditions in Lancaster Sound; and (iii) weak reducing conditions in the Beaufort Shelf, Canadian Archipelago and Davis Strait.

5.2. Controls on the vertical distributions of authigenic phases of Mo, Cd, U and Re

5.2.1. Mo

During early diagenesis, dissolved Mo becomes incorporated in the solid-phase under both oxidizing and reducing conditions (cf., Calvert and Pedersen, 1993; Crusius et al., 1996; Chaillou et al., 2002; Morford et al., 2005). Under oxidizing conditions, the adsorption of Mo to Mn oxyhydroxides appears to be the most recognized scavenging mechanism for incorporating authigenic Mo (Mo_A) into marine sediments (e.g., Sundby et al., 2004). In our sediments, the highly significant correlation between MoA and Mn_A in both our compiled data set for the NAAM $(r^2 = 0.90, p < 0.001, n = 178)$ and within the Mnenriched layers of 16 individual cores ($r^2 > 0.56$, p < 0.03) (Fig. 5) provides supplementary evidence supporting such The mechanism. average Mo/Mn $(0.001~{\rm g~g^{-1}} \pm 0.001~{\rm g~g^{-1}}, n = 178)$ in the Arctic's oxic sediments is, furthermore, typical of the ratio (0.002 g g⁻¹) observed worldwide in Mn oxide rich sediments and ferromanganese deposits (Shimmield and Price, 1986).

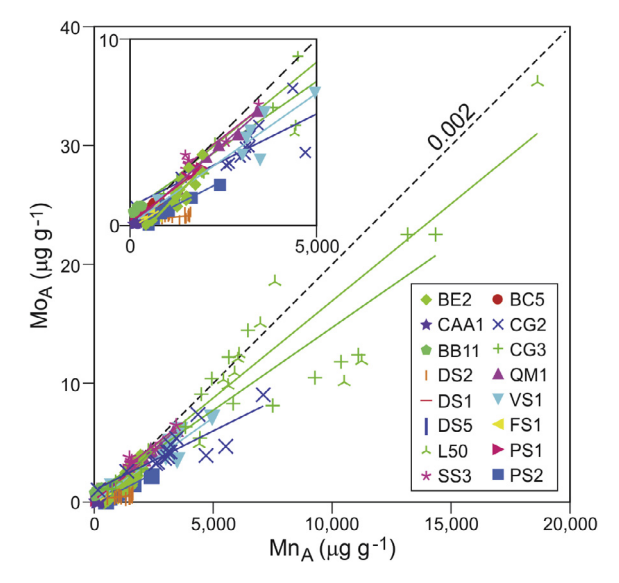


Fig. 5. Relationships between Mo_A and Mn_A in sediment samples from the Mn enriched surface layer. The solid lines indicate statistically significant relationships. The dashed line shows the typical ratio $(0.002~g~g^{-1})$ observed worldwide in Mn oxide rich sediments and ferromanganese deposits (Shimmield and Price, 1986).

The exact mechanism by which dissolved Mo becomes fixed under reducing conditions in marine sediments remains a subject of discussion (e.g. Helz and Adelson, 2013; Chappaz et al., 2014). It is generally accepted that dissolved Mo, which exists as MoO₄²⁻ in oxygenated waters, is initially converted to tetrathiomolybdate in the presence of sufficiently high concentrations of HS⁻ (Helz et al., 1996; Erickson and Helz, 2000), and that Mo_A subsequently accumulates as a Mo-Fe-S solid, the composition of which remains imprecisely defined (e.g., Helz et al., 1996; Erickson and Helz, 2000; Helz and Adelson, 2013). Dahl et al. (2013) have recently identified Mo(IV)-S compounds in euxinic lake sediments but their observations need corroboration before they can be generalized. On the other hand, Chappaz et al. (2014) concluded that substitution of Fe atoms by Mo atoms during the formation of pyrite in black shales is of relatively minor significance. Regardless of the exact removal mechanisms of MoA, the concomitant increases in Mo and S (both S_{tot} and S_{red}) with depth in Arctic sediments, beginning from the sediment-water interface in the cores from Bering-Chukchi shelf (Fig. 2a) and shallow Barrow Canyon (Fig. 2b), or below the base of the Mn-rich surface layer in many cores from the other regions (Fig. 2b-d), provide strong evidence of Mo fixation under reducing conditions.

For the 13 cores from the North Bering-Chukchi shelf, Barrow Canyon, Lancaster Sound, and Beaufort Shelf (CG1), the slopes of the Mo_A-S_A relationships are similar across the regions: statistically significant relationships (slopes 0.59–1.74, $r^2 = 0.35$ –0.91, and p < 0.003) between authigenic Mo (Mo_A) and S (S_A) are observed. For three cores (SLIP1, UTN7 and BC5), there are sediment sections with anomalously low MoA concentrations relative to SA that we have treated as outliers in the regressions (see open symbols in Fig. 6). Of these cores, UTN7 is the most interesting because it clearly contains an upper section extending down to about 30 cm depth that has a much shallower slope (Fig. 6). Based on the ²¹⁰Pb profile (Kuzyk et al., 2013; Table 1) and the Re profile, we suspect that this sediment has been mixed deeply, from which we infer that the slope of MoA to SA reflects mixing rather than in-situ sequestration. It is noteworthy that positive intercepts for MoA at S_A = 0 are found for sediments that have Mn surface enrichments (most sediments outside the North Bering-Chukchi shelf). This observation is consistent with surface Mn-associated Mo enrichments facilitating authigenic Mo accumulation in reducing sediments below the Mnenriched layer (cf., Scholz et al., 2013). In contrast to other studies that have found correlations between Mo and OC concentrations in reducing sediments (cf., Algeo and Lyons, 2006), our sediments exhibit no such relationship within individual cores and a weak relationship for the entire data set $(r^2 = 0.22, p < 0.001, n = 353, core BC3)$ excluded).

5.2.2. Cd

Upper portions of the Cd profiles, in which concentrations are slightly elevated in surface sediments and decrease within the oxic zone (see, for example, VS1, PS1, CG2), are interpreted as representing biogenic supply of particulate

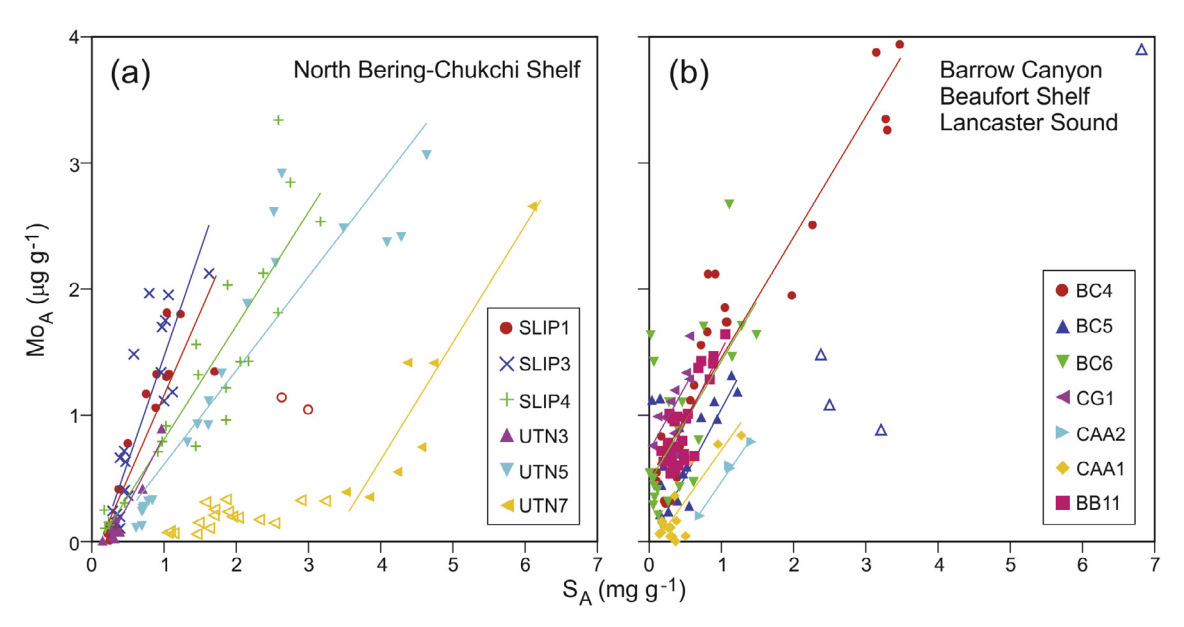


Fig. 6. Relationships between authigenic sulphur (S_A) and authigenic Mo (Mo_A) in the sediments from the North Bering–Chukchi Shelves (a) and in sediments below the Mn enriched surface layer from Barrow Canyon, Beaufort Shelf, and Lancaster Sound (b). All the listed cores exhibited statistically significant relationships. Open symbols indicate outliers that were excluded from regression analyses.

Cd to surface sediments, which is being released to porewater as organic matter (OM) is aerobically degraded (Gendron et al., 1986; Gobeil et al., 1987). In the upper sediment layers of our cores (i.e., above the Cd minimum), Cd_A and OC are highly correlated, both within nine individual cores ($r^2 = 0.50$ –0.95) and in the compiled data set ($r^2 = 0.85$, p < 0.001, n = 167). The Cd_A:OC ratios implied by the slopes of the relationships as well as the Cd_A:OC ratios in upper portions of most of the cores (Fig. 7) are similar to or slightly less than the Cd_A:OC ratio reported for particulate marine OM (\sim 2–3 µmol mol⁻¹) (Rosenthal et al., 1995b; Morel and Malcom, 2005).

Increases in Cd with depth beginning below the concentration minima in the shallow subsurface are nearly ubiquitous in the sediments (Fig. 2) and are interpreted as authigenic Cd (Cd_A) accumulation. In support of this interpretation, Cd_A:OC ratios in deep sediment layers generally are greater than the Cd_A:OC ratios in upper portions of the cores and, in many cases, exceed the particulate marine OM ratio ($\sim 2-3 \,\mu\text{mol mol}^{-1}$) (Rosenthal et al., 1995b; Morel and Malcom, 2005) (Fig. 7). Furthermore, significant positive Cd_A-S_A relationships are found in the deeper sediment sections of seven individual cores ($r^2 = 0.30-0.66$). The significant Cd_A-S_A relationships in the sediments are consistent with precipitation of CdS providing the primary removal mechanism for Cd in these sediments (cf., Rosenthal et al., 1995b). However, the noisiness of the Cd_A-S_A relationships, compared to those of Mo_A $(r^2 = 0.30 - 0.66 \text{ vs. } r^2 > 0.73)$, indicate that factors other than sulphide availability influence authigenic Cd accumulation in these sediments. Variation in Cd supply is likely important, in view of the element's biological activity and hence low concentrations in productive shelf waters (cf., Little et al., 2015). In particular, low maximum Cd_A:OC ratios in deep sediments in the North Bering-Chukchi shelf,

Barrow Canyon, and Beaufort Shelf (CG2 excepted) compared to the Archipelago (FS1 excepted) and Davis Strait $(1.1-4.0 \, \mu \text{mol mol}^{-1} \, \text{vs.} \, 3.5-13.9 \, \mu \text{mol mol}^{-1}; \, \text{Fig. 7}) \, \text{sug-}$ gest Cd supply is limited in the western part of the study area but not further east (with the exception of Lancaster Sound). The statistically significant Cd_A intercepts at $S_A = 0 \ (\sim 0.1 \ \mu g \ g^{-1})$ imply that a small amount of particulate Cd is directly transferred from the oxic to suboxic zones or that Cd released to porewater from OM degradation in surface sediments diffuses downward and enhances the supply of Cd available to precipitate as CdS in the presence of dissolved sulphide. The core (UTN5) in which the Cd_A intercept is highest $(0.20 \,\mu g \,g^{-1})$ is from the Chukchi shelf, where the shallow, productive waters are probably low in Cd due to biological uptake. Thus, continuous supply of Cd from OM degradation may become increasingly important for enhancing authigenic Cd enrichment in regions like this one, where bottom water concentrations of Cd are low (provided dissolved sulphide is not limiting within the sediment column).

5.2.3. U

Although U concentrations in the Mn-rich layers of the cores are relatively constant and lower than values in deeper sediment sections (Fig. 2), the concentrations often slightly exceed $U_{\rm litho}$ in the cores, consistent with a small supply of U being scavenged from the water column and delivered to the sediment as part of the particulate flux (i.e., particulate non-lithogenic U; Anderson, 1982; Zheng et al., 2002a). While most previous studies have found no evidence of Mn oxides influencing the distribution of U (Klinkhammer and Palmer, 1991; Morford et al., 2005; McManus et al., 2006), here, the U_A concentrations in the Mn enriched sediment layer are correlated with Mn_A concentrations within three cores (VS1, FS1, DS2; $r^2 > 0.52$,

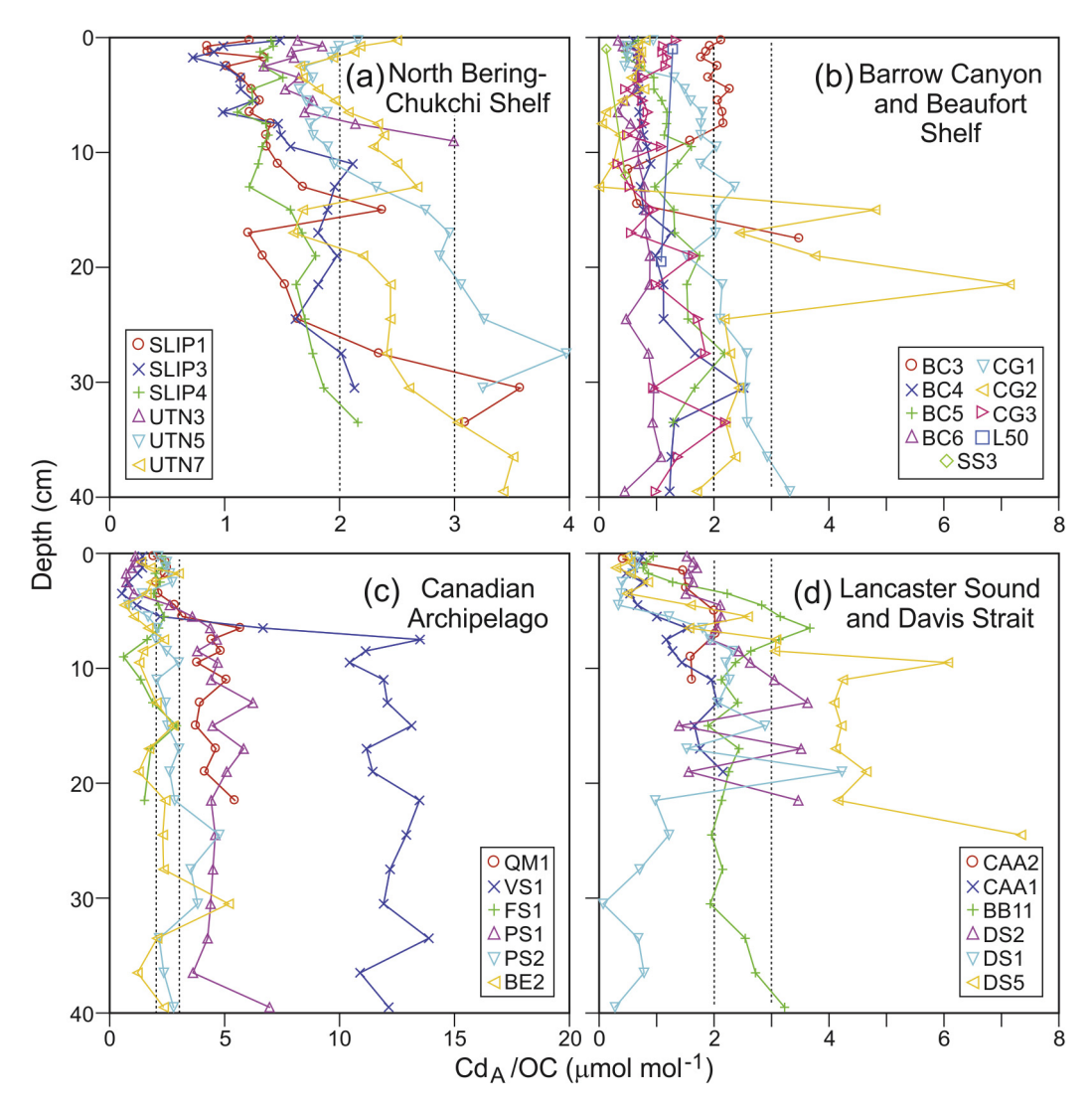


Fig. 7. Profiles of molar Cd_A :OC ratios in the cores. Dotted vertical lines represent the Cd_A :OC ratio reported for particulate marine OM (\sim 2–3 µmol mol⁻¹) (Rosenthal et al., 1995; Morel and Malcom, 2005).

p < 0.002; not shown). This result supports the findings of Morford et al. (2007) that U can cycle to a limited extent with Mn oxides. In the same three cores, UA concentrations in oxic sediments are also weakly correlated with OC $(r^2 = 0.40 - 0.42, p < 0.004)$. U-OC correlations have been observed in a variety of oceanographic settings and may reflect U associating with particulate organic carbon in the water column, perhaps through surface complexation or perhaps biological uptake (e.g., Zheng et al., 2002a). The influence of this process here is obviously weak. In view of the limited U_A-Mn_A and U_A-OC relationships and also the low U_A concentrations in oxic sediments compared to subsurface values (Fig. 2), we conclude that the major source of U for authigenic enrichment in subsurface sediments here is downward diffusion of soluble U(VI) from the water column.

The relatively abrupt increases in U concentration near the base of the Mn enriched layer in many of the cores

(see, for example, cores VS1, PS1, BB11, BC5, CG2; Fig. 2) are consistent with downward diffusing U(VI) being converted to relatively insoluble U(IV) where it encounters weakly reducing conditions in the sediments (Cochran et al., 1986; Gariépy et al., 1994; McManus et al., 2005). The occurrence of strong U enrichments in several cores having very weak Mo and Cd enrichments, including cores BC5, DS1 and DS5, implies that authigenic U precipitates even in very weakly reducing conditions in the sediments. It is also striking that the highest U_A concentrations (4-5 μg g⁻¹) are present not in cores from the Chukchi Shelf and Barrow Canyon (as was the case for Mo and to some extent Cd) but rather in cores from the Beaufort Shelf, Canadian Archipelago, and Lancaster Sound (Fig. 2). Similarly, the largest UA inventories are present in cores from the Canadian Archipelago and Lancaster Sound (Fig. 4). The implication is that maximum UA concentrations (and inventories) do not correspond to the relative ordering of sediments according to their 'reducing intensity', as inferred from Mn, S_{red} and S_{tot} . This result suggests strikingly different controls on U_A accumulation than those on Mo_A and Cd_A . Considering that many of the cores with high U concentrations (VS1, BB11) have low sedimentation rates (~ 0.05 cm yr⁻¹; Table 1), one of the controls on U_A accumulation could be slow precipitation kinetics, which leads to higher concentrations in slowly-accumulating sediments (Sundby et al., 2004; Kuzyk et al., 2011).

U profiles in Bering–Chukchi shelf sediments are enigmatic in that U_A enrichment does not begin until $\sim\!20$ cm despite reducing conditions commencing almost at the sediment surface and Mo_A beginning to accumulate within about 10 cm of the sediment surface (Fig. 2). A possible explanation is remobilization of U_A as a result of deep, intense biomixing (Table 1) that at times exposes U_A to dioxygen (cf., Cochran et al., 1986; Zheng et al., 2002b; Morford et al., 2009a,b). The contrast between U_A and Mo_A may arise from the latter being more resistant to remobilization or, more likely, to its recycling to Mo_A when reducing conditions are re-established (e.g., see Crusius and Thomson, 2000; Helz and Adelson, 2013).

5.2.4. Re

The pronounced increases in Re concentration with depth beginning below the Mn-enriched layer are interpreted as reflecting authigenic Re enrichment, wherein Re is dissolved in the presence of O_2 but enters the solid phase under weakly reducing conditions (Crusius et al., 1996; Crusius and Thomson, 2003). Dissolved Re, which occurs in oxic seawater as the unreactive perrhenate anion (ReO₄: Bruland and Franks, 1983), presumably diffuses into sediments from the bottom water and precipitates where weakly reducing conditions are encountered in the sediments, although the removal pathway for Re is still poorly understood (cf., Helz and Adelson (2013)). The insoluble species of Re accumulating in reducing sediments possibly include rhenium oxide (ReO₂), dirhenium heptasulphide (Re₂S₇(s)) or rheniite (ReS₂) (Nameroff et al., 2002; Tribovillard et al., 2006; Chappaz et al., 2008).

An alternative hypothesis presented recently is that Re coprecipitates in a Fe-Mo-S colloidal phase in sulphidic sediments, perhaps approximating Fe₅Mo₃S₁₄ (Helz and Dolor, 2012; Helz and Adelson, 2013). In our sediments, there are strong correlations between authigenic Re and Mo in all of the sediments with relatively strong reducing conditions (Fig. 8), as would be expected under a coprecipation mechanism. However, the slopes of the Re_A-Mo_A relationships differ significantly among the various shelf regions, with Lancaster Sound greatly exceeding the North Bering-Chukchi shelf and Barrow Canyon. Furthermore, in all of the sediments, the apparent Re_{Δ}/Mo_{Δ} ratios lie well above the expected atomic ratio for the coprecipitation phase, assuming equilibration with dissolved Mo and Re in their typical seawater molar ratio of 10⁻⁴ (Helz and Adelson, 2013). We conclude that the accumulation of both elements may be governed by diffusion into the sediments thus giving rise to correlation in ReA and MoA concentrations; however, the elements seem to have independent removal mechanisms in these sediments. Further evidence

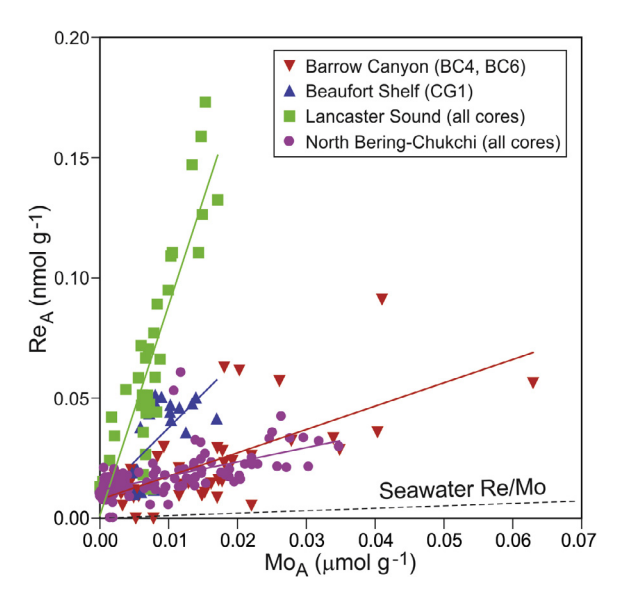


Fig. 8. Relationships between authigenic Mo (Mo_A) and Re (Re_A) concentrations in selected cores from all regions, excluding samples from the Mn enriched surface layer.

of independent mechanisms is provided by the rather abrupt increase in Mo_A concentrations in near-surface sediment layers in the Bering–Chukchi shelf cores, in contrast to gradually increasing Re_A concentrations with depth (Fig. 2; note UTN7 is an exception).

Although the pronounced Re_A enrichments in the sediments all begin below the Mn-enriched layers in our cores, we note that the minimum Retot concentrations in the cores are generally higher than typical crustal values of 0.05-0.5 ng g⁻¹ for this element (Esser and Turekian, 1993; Wedepohl, 1995; Peucker-Ehrenbrink and Jahn, 2001; McLennan, 2001; Borchers et al., 2005). Indeed, in all of the cores from the western part of the study area and Lancaster Sound, the minimum Retot concentrations are 2- 3 ng g^{-1} (Fig. 2). This apparent enrichment cannot be due to the interaction of ReO₄ with Mn oxides (Crusius et al., 1996; Morford et al., 2005) because the profiles of Re and Mn bear no resemblance to one another (Fig. 2). Biogenic supply may be ruled out because Re is not required by phytoplankton, nor do sediment profiles show a subsurface decrease in Re concentrations (Fig. 2) as expected for a metal associated with OM (cf., profiles of Cd in Gobeil et al., 1987). Upward biomixing of ReA from the suboxic zone to the oxic zone followed by slow dissolution of Re_A could explain the trends in cores with intense mixing but most of the Lancaster Sound cores have only 1-cm thick surface mixed layers (Table 1). Another possibility is that many of the cores may have reducing microenvironments created by episodic labile OC fluxes despite longterm conditions characterized by low OC fluxes. This hypothesis is supported by the observation that minimum Retot concentrations comparable to typical crustal values are found only in cores with low S_{red} concentrations (10-16 μg g⁻¹) irrespective of water depths (i.e., BE2, FS1, PS2 and DS2).

5.3. The relationship between surface Mn enrichment and Cd_A , U_A and Re_A profiles

In most cores the profiles of Cd_A , U_A and Re_A bear striking similarities, closely paralleling one another at several sites (Fig. 2). In cores with only a thin surface layer of Mn enrichment, Cd_A , U_A , and Re_A beneath that layer remain relatively low and constant, or even decrease slightly. Where the Mn_A layer is thicker with higher Mn_A enrichment, Cd_A , U_A and Re_A increase abruptly beneath that layer from minimum to maximum values, which are maintained to the bottom of the core.

Two extreme cores – CG2 in the Mackenzie Shelf and VS1 in the Canadian Archipelago – in which the Mn layer was >7 cm and Mn enrichments exceeded 5 mg g $^{-1}$, contained the most elevated concentrations for Cd $_{\rm A}$ (>0.9 μg g $^{-1}$), U $_{\rm A}$ (>5 μg μg^{-1}) and Re $_{\rm A}$ (>15 ng g $^{-1}$) (Fig. 2) observed in our study. Lastly, for the 12 cores having negligible Mn enrichment in surface sediments but elevated S $_{\rm A}$, the concentrations of Cd $_{\rm A}$, U $_{\rm A}$, and Re $_{\rm A}$ attain relatively high values immediately at the sediment surface, but the rate of increase with depth is much lower than in most cores characterized by Mn surface enrichment.

Table 3 Authigenic element (S_A , Mo_A , Cd_A , U_A , Re_A) accumulation rates calculated from sedimentation rates and authigenic concentrations deep in the cores (>30 cm).

Region and core number	$S_A (mg cm^{-2} yr^{-1})$	$Mo_A~(\mu g~cm^{-2}~yr^{-1})$	$Cd_{A} \ (\mu g \ cm^{-2} \ yr^{-1})$	$U_A \ (\mu g \ cm^{-2} \ yr^{-1})$	$Re_A (ng cm^{-2} yr^{-1})$
North Bering Sea Shelf					
SLIP1	1.10	0.42	0.10	0.92	4.11
SLIP3	0.54	0.70	0.05	0.37	1.48
SLIP4	0.76	0.65	0.06	0.42	2.39
Average (SD)	0.80 (0.28)	0.59 (0.15)	0.07 (0.03)	0.57 (0.30)	2.66 (1.34)
Chukchi Sea Shelf					
UTN3	1.01 ^a	0.87^{a}	0.10^{a}	0.46^{a}	0.89^{a}
UTN5	1.30	0.86	0.10	0.44	0.89
UTN7	1.42	0.74	0.11	0.43	0.78
Average (SD)	1.24 (0.21)	0.82 (0.07)	0.11 (0.01)	0.44 (0.02)	0.85 (0.07)
Barrow Canyon					
BC3	0.26^{a}	0.05^{a}	0.15^{a}	0.25^{a}	0.44^{a}
BC4	0.53	0.58	0.03	0.34	1.49
BC5	0.23	0.13	0.01	0.09	0.30
BC6	0.07	0.14	0.01	0.12	0.56
Average (SD)	0.27 (0.19)	0.22 (0.24)	0.05 (0.07)	0.20 (0.11)	0.70 (0.54)
Beaufort Shelf					
CG1	0.07	0.18	0.05	0.34	1.64
CG2	0.00	0.05	0.02	0.08	0.92
CG3	0.00	0.08	0.01	0.05	0.61
L50	0.00	0.07	0.01	0.04	0.19
SS3	0.00	0.04	0.01	0.08	0.53
Average (SD)	0.01 (0.04)	0.08 (0.06)	0.02 (0.02)	0.12 (0.13)	0.78 (0.55)
Canadian Archipelago					
QM1	0.00	0.11	0.03	0.30	0.60
VS1	0.00	0.03	0.03	0.16	0.59
FS1	0.00	0.00	0.00	0.07	0.12
PS1	0.00	0.00	0.01	0.07	0.43
PS2	0.00	0.00	0.01	0.13	0.04
BE2	0.00	0.00	0.01	0.13	0.02
Average (SD)	0.00 (0.00)	0.02 (0.05)	0.02 (0.01)	0.14 (0.08)	0.30 (0.27)
Lancaster Sound					
CAA2	0.23	0.09	0.03	0.25	1.03
CAA1	0.29	0.15	0.04	0.51	2.15
BB11	0.05	0.05	0.02	0.22	2.89
Average (SD)	0.19 (0.13)	0.10 (0.05)	0.03 (0.01)	0.33 (0.16)	2.02 (0.94)
Davis Strait					
DS2	0.00	0.00	0.00	0.00	0.00
DS1	0.06	0.00	0.00	0.04	0.04
DS5	0.02	0.00	0.01	0.12	1.46
Average (SD)	0.03 (0.03)	0.00 (0.00)	0.01 (0.01)	0.06 (0.05)	0.50 (0.83)

^a In these short cores, concentrations at depth were estimated by linearly extrapolating from the deepest available samples.

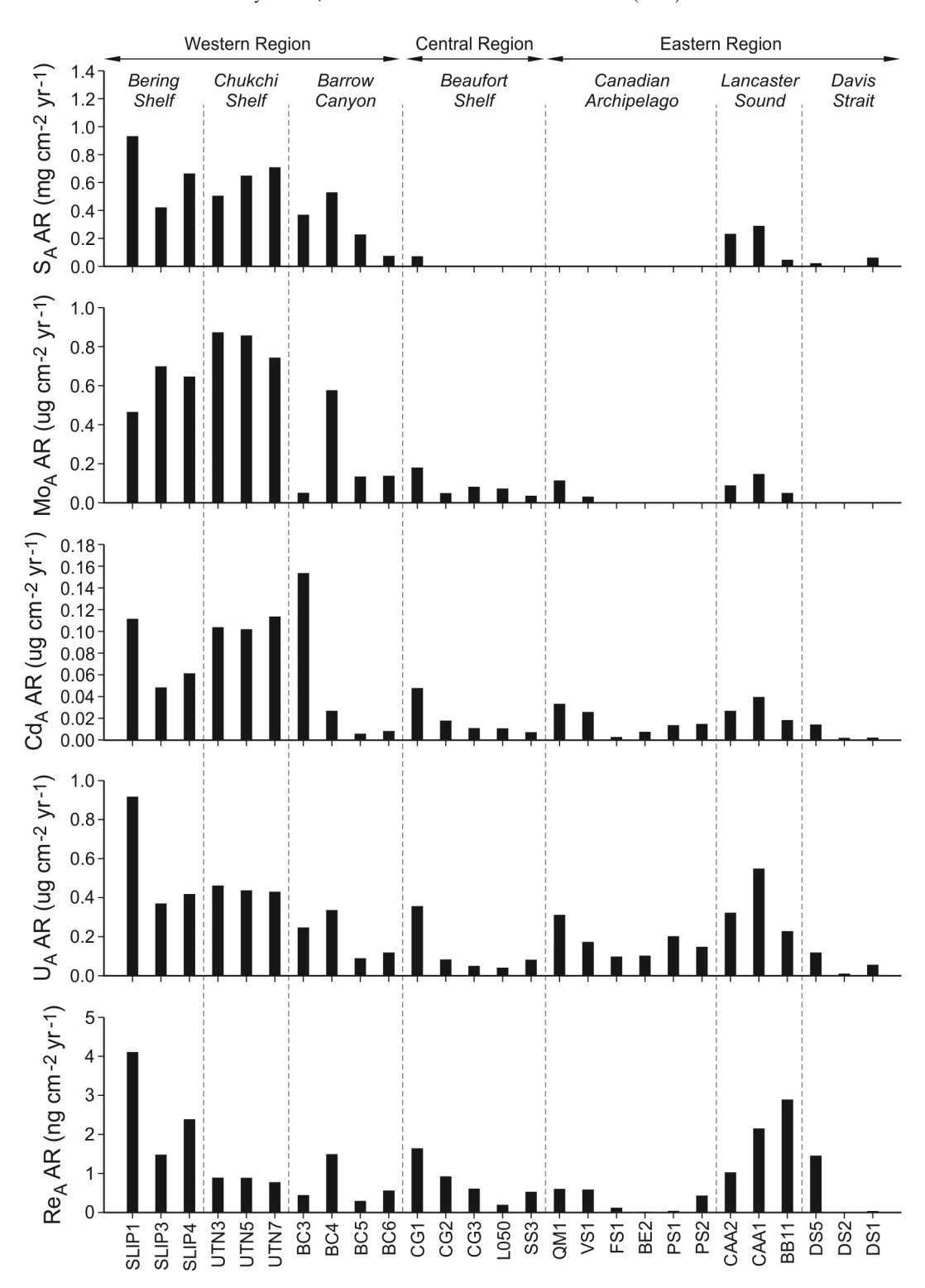


Fig. 9. Average authigenic element (S_A, Mo_A, Cd_A, U_A, Re_A) accumulation rates in the sediments across the seven subregions of the North American Arctic margin as determined by multiplying the sedimentation rates and the authigenic concentrations at the bottom of the cores.

5.4. Trace element accumulation rates in reducing sediments

Average accumulation rates for S_A, Cd_A, Mo_A, U_A, and Re_A in each core may be estimated as the product of the sedimentation rate and the concentration of the authigenic

elements measured at depth in the cores (>30 cm). These calculations provide the ultimate accumulation rates of the authigenic component of the elements, assuming that below ~ 30 cm depth concentrations remain constant. We have chosen this approach because, in many cores, espe-

cially those with deep biomixing, the concentrations of the elements strongly increase with depth (Fig. 2). In the cases of the two short cores (UTN3 and BC3), concentrations at depth are estimated by linear extrapolation of the depthconcentration relationship exhibited by the deepest available sections. The sediment accumulation rates, based on ²¹⁰Pb and ¹³⁷Cs profiles, are taken from Kuzyk et al. (2013) or newly derived (SLIP-1, -3, -4, UTN5, L50, SS3) following the same methods described in that reference. Unfortunately, due to the setting (biomixing, low ²¹⁰Pb fluxes). ²¹⁰Pb-derived sedimentation rates are not very well constrained for sediments from the Bering-Chukchi shelves (Table 1). For a few vigorously biomixed sediments that could not be dated at all using ²¹⁰Pb (UTN3, UTN7, and BC3), we apply sedimentation rates determined in nearby cores (Table 1). We note that these rates lie within the range of previously reported sedimentation rates for the eastern Chukchi Shelf (0.08-0.32 g cm⁻² yr⁻¹; Baskaran and Naidu, 1995).

Accumulation rates for SA, MOA, CdA, UA and ReA for the 27 core sites are presented in Table 3 and illustrated by region in Fig. 9. Accumulation rates for SA, MoA, CdA, UA and Re_A all show a clear regional pattern, with highest rates in the Bering-Chukchi shelves and the shallower sites in Barrow Canvon, moderate rates in Lancaster Sound, and generally low rates in the Beaufort Shelf, Canadian Archipelago and Davis Strait (Fig. 9). There are some subtle differences in the relative rates of accumulation among the various redox elements, for example, SA and MoA have accumulation rates of essentially zero in the Beaufort Shelf, Canadian Archipelago and Davis Strait regions, whereas Cd_A, U_A and Re_A have low but non-zero rates in these regions. The accumulation rates of UA and ReA in Lancaster Sound sediments are similar in magnitude to the rates in the Bering-Chukchi shelves (Fig. 9).

Despite these subtle differences, the regional patterns – high in the Bering-Chukchi shelves and Barrow Canyon, medium in Lancaster Sound, and low in the other regions - are so consistent across all the redox elements that clearly the major sources of variation in the trace element accumulation rates are organized by region. The regional patterns in accumulation rate also agree with the regional differences in 'reduction intensity'. In view of the well-oxygenated bottom waters along the NAAM margin, the spatial variability in redox conditions and authigenic element accumulation rates must be governed by the supply of labile carbon to the seabed. In support of this assertion are strong relationships between the accumulation rates and vertical carbon flux, estimated from regional primary production values and water depth at the coring sites (Fig. 10). Specifically, we estimated the vertical flux at our coring sites using a simple empirically-derived model, J = 20PP/z, where J is the flux of carbon in units of gC m⁻² yr⁻¹, PP is annual primary production in units of gC m⁻² yr⁻¹ and z is water depth in m (Suess, 1980; Berger et al., 1987; Bishop, 1989; Hulth et al., 1994). We used the average annual primary production values for the various regions as reported in Sakshaug (2004) and Grebmeier et al. (2006), i.e., 460 gC m⁻² yr⁻¹ for the Chukchi Shelf, 360 gC m⁻² yr⁻¹ for the Bering Shelf, 430 gC m⁻² yr⁻¹ for Barrow Canyon,

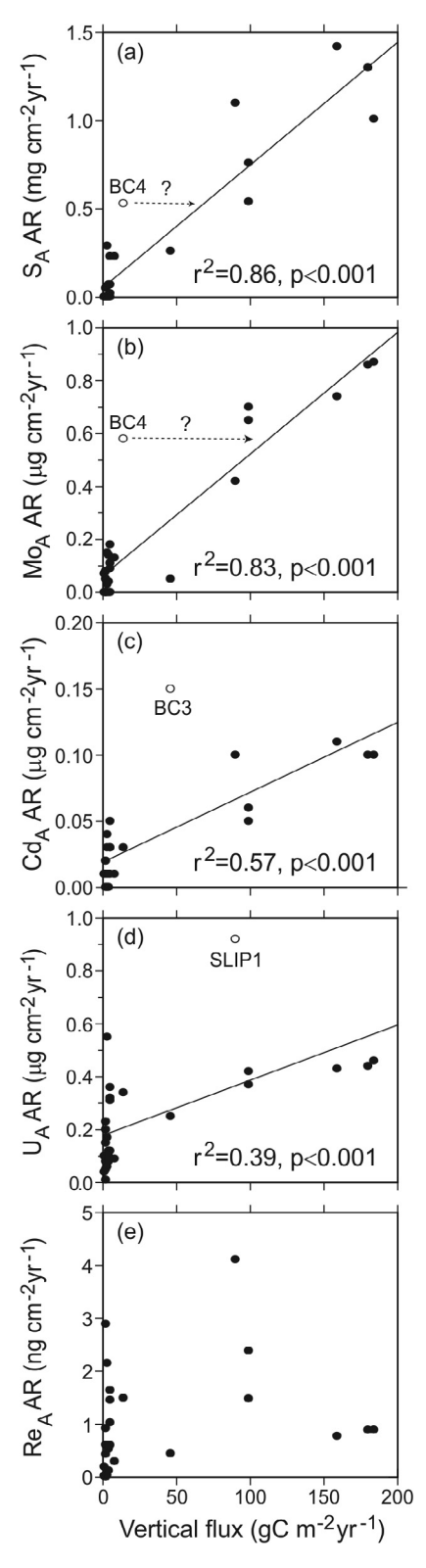


Fig. 10. Average authigenic element (S_A, Mo_A, Cd_A, U_A, Re_A) accumulation rates plotted against the vertical carbon flux at each site as estimated from regional primary production values and water depth (see text for details). The open circles in panels a, b and c represent outliers (cores BC3 and BC4).

 $50~{\rm gC~m^{-2}~yr^{-1}}$ for the Beaufort Shelf, $30~{\rm gC~m^{-2}~yr^{-1}}$ for the Canadian Archipelago, and $90~{\rm gC~m^{-2}~yr^{-1}}$ for all remaining regions. Note that $90~{\rm gC~m^{-2}~yr^{-1}}$ is the reported value for Baffin Bay but in the absence of more specific subregional data, we apply this value to both Lancaster Sound and Davis Strait.

Plots of the accumulation rates for S_A , Mo_A , Cd_A , U_A , and Re_A in the cores against the labile OC flux (Fig. 10) show strong significant relationships for S_A ($r^2=0.86$, p<0.001) and Mo_A ($r^2=0.83$, p<0.001) and noisier but still significant relationships for Cd_A and U_A ($r^2=0.57$ and 0.39; Fig. 10). The noisiness of these latter relationships and the lack of significant relationship for Re_A might reflect the fact that Re_A and U_A precipitate in very weakly reducing sediments or even weakly reducing microenvironments, the existence of which depends on many factors (e.g., degree of sediment mixing, temporal distribution of the OC flux) besides annual labile OC flux. Quite a bit of the scatter is due to unusually high U_A and Re_A accumulation rates in sediments at relatively deep sites.

Core BC4 from Barrow Canyon is an outlier in several of the plotted relationships (cf., Fig. 10a and b). The SA and MoA accumulation rates for BC4 imply a vertical flux at this site on the order of 100–150 gC m⁻² yr⁻¹, rather than the ~ 14 gC m⁻² yr⁻¹ estimated from regional primary production values and the site's water depth (499 m). Although OC values at this site are no higher than at nearby sites, the sediment accumulation rate is higher and may ultimately be driving higher vertical carbon fluxes and thus higher SA and MoA accumulation rates. This result is consistent with the notion that deposition of shelf-derived materials is enhanced in the upper and middle (100-500 m water depth) part of Barrow Canvon (Darby et al., 2009; Kuzyk et al., 2013). Furthermore, the result indicates that the deposited materials are labile, which implies a rapid transport mechanism that reduces the vertical flux attenuation generally associated with zooplankton grazing. Among the various particle transport mechanisms proposed to operate in this region, brine enriched winter density flows (Weingartner et al., 2005; Williams et al., 2008) seem more likely to promote the deposition of unexpectedly labile material at depth than do resuspension of shelf material and midwater transport (Lepore et al., 2009) or eddies (O'Brien et al., 2011).

Although variation in vertical carbon flux (and thus labile OC forcing) clearly explains most of the variation in trace element accumulation rates among Arctic margin sediments, there are two other factors that could influence these rates. One is the supply of terrestrial organic material, which is strongest in the Beaufort Shelf (near the Mackenzie River), followed by the Bering-Chukchi shelves and Barrow Canyon (perhaps because of Yukon River influence and/or erosion of coastal and/or sub-seafloor peat) (Goñi et al., 2013). To test for the influence of terrestrial organic matter on trace element accumulation rates, we take the residuals from the linear regression relationships of accumulation rate and vertical flux and regress them against the percent of terrestrial vascular plant input at each site (Fig. 10) (cf., Hebert and Keenleyside, 1995). This value was derived by Goñi et al. (2013) from the results of Prin-

cipal Components Analysis (PCA) of biomarker and bulk isotopic data for the surface sediments of the same (25) cores examined here (Goñi et al., 2013). Using this multiproxy index of vascular plant input, we find a statistically significant relationship with the residuals from the vertical flux vs. Mo_A accumulation rate regression ($r^2 = 0.19$, p = 0.022, BC3 excluded as outlier) (Fig. 11). We do not find significant relationships between these regression residuals and other properties such as sedimentation rate. The significant relationship between the residuals and percent vascular plant input suggests that terrestrial vascular plant inputs may contribute significantly, in addition to the vertical (marine-derived) carbon flux, to supporting sedimentary carbon turnover and hence the accumulation of redoxsensitive elements in Arctic margin sediments. This result is not entirely surprising because, although terrestrial OC is generally considered much less reactive than marine OC (Prahl et al., 1994; Burdige, 2005), it has been shown in recent studies to degrade more rapidly than previously thought and to represent an important overall contributor to metabolism in Arctic margin areas (Sánchez-García et al., 2011; Vonk et al., 2012). In the Laptev and East Siberian Arctic margin areas, Sánchez-García et al. (2011) estimated a first-order degradation rate constant for terrestrial particulate OC of $1.4 \pm 0.9 \text{ yr}^{-1}$, which corresponds to a calculated half-life of only ~ 0.5 yrs. In the Beaufort Shelf region, Goñi et al. (2005) estimated from sediment OC/surface area ratios that as much as 25% of the ancient OC discharged by the Mackenzie River ($\sim 0.35 \times 10^9 \text{ kg yr}^{-1}$) is lost annually from sediment particles prior to burial in the outer shelf. With the large magnitude of terrestrial OC export by the Mackenzie River and this degree of remineralization, the potential is there for terrestrial OC to sig-

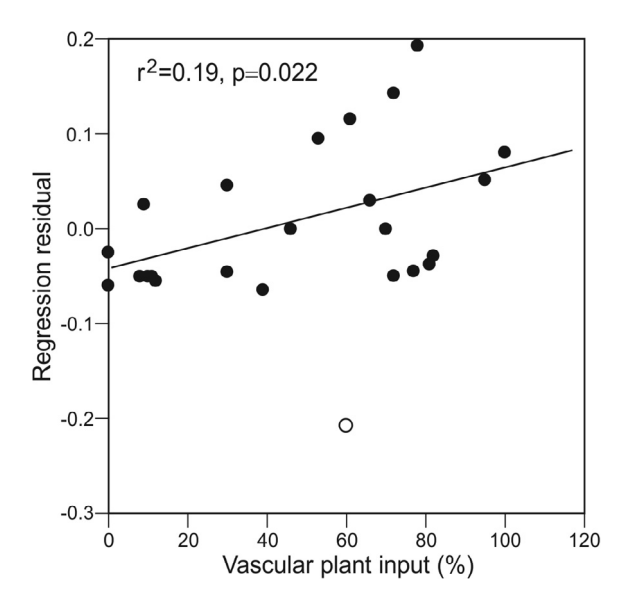


Fig. 11. Regression residuals from Mo_A accumulation rates vs. vertical carbon flux (see Fig. 10b) plotted against relative percent terrestrial vascular plant inputs, as derived from principal components analysis (PCA) of organic geochemical data for surface sediment samples (Goñi et al., 2013). The open circle represents an outlier (core BC3) that was removed from the regression.

nificantly contribute to sedimentary carbon turnover and trace element accumulation in the Beaufort Shelf region, at least.

The other factor that can be important in controlling trace element accumulation rates is activity of macrobenthos, including bioturbation and pore water irrigation in margin sediments that underlie well-oxygenated bottom waters (Morford et al., 2007, 2009a,b). For instance, Morford et al. (2009a) demonstrated that U_A accumulation rates were lower in sediments that underlie waters with high bottom water O₂ content compared to those predicted from rates in areas with low bottom water O₂ content, presumably reflecting oxidation and loss of U from the solid phase via irrigation and/or bioturbation in the well-oxygenated areas. Bioturbation and porewater irrigation are both intense in Bering-Chukchi shelf sediments (Clough et al., 1997; Kuzyk et al., 2013), with SMLs (as interpreted from 210 Pb profiles) as thick as ~ 10 cm in some cores from these regions, compared to ~1-2 cm in most other regions (Table 1). In the case of UTN7, which has the deepest biomixing, oxidation and loss of Mo appears to have been significant based on the abnormally low Mo accumulation in the top ~ 20 cm of that core (Fig. 6). Partial oxidation and loss of Re resulting from deep biomixing and porewater irrigation may also explain in part the low Re/Mo ratios in the North Bering-Chukchi shelf sediments (Fig. 8) relative to the expected ratio assuming equilibration with dissolved Mo and Re in their typical seawater ratio (Helz

and Adelson, 2013). At the same time, we find no relationship here between the flux-adjusted authigenic element accumulation rates and the thickness of the SML across our cores. It may be that the effects of bioturbation and porewater irrigation affect the very nature (i.e., slopes) of the relationships we observe between vertical flux and accumulation rate because all of the high flux sites have relatively thick SMLs implying strong effects of bioturbation and porewater irrigation. What is needed is a comparison of sites with similar (high) vertical carbon fluxes but a wide range in bottom water oxygen levels and thus macrobenthos activity (cf., Morford et al., 2009a). In Fig. 12, UA accumulation rates for the Bering-Chukchi shelf are plotted together with the literature results for UA accumulation rates and carbon flux compiled by Morford et al. (2009a), as well as some additional recent results for Hudson Bay (Kuzyk et al., 2011) and the Strait of Georgia (Macdonald et al., 2008). Following the example of Morford et al. (2009a,b), we plot data from locations with low bottom water O₂ levels (<150 μM; open symbols) and high bottom water O_2 levels (>150 μM ; closed symbols) separately. We find that the UA accumulation rates are indeed somewhat lower in the Bering-Chukchi shelf sediments compared to those predicted from relationships developed from locations with poorly oxygenated waters (Fig. 12). However, the U_A accumulation rates for Bering-Chukchi shelf sediments do not appear to be as strongly affected by bioturbation and/or bioirrigation as

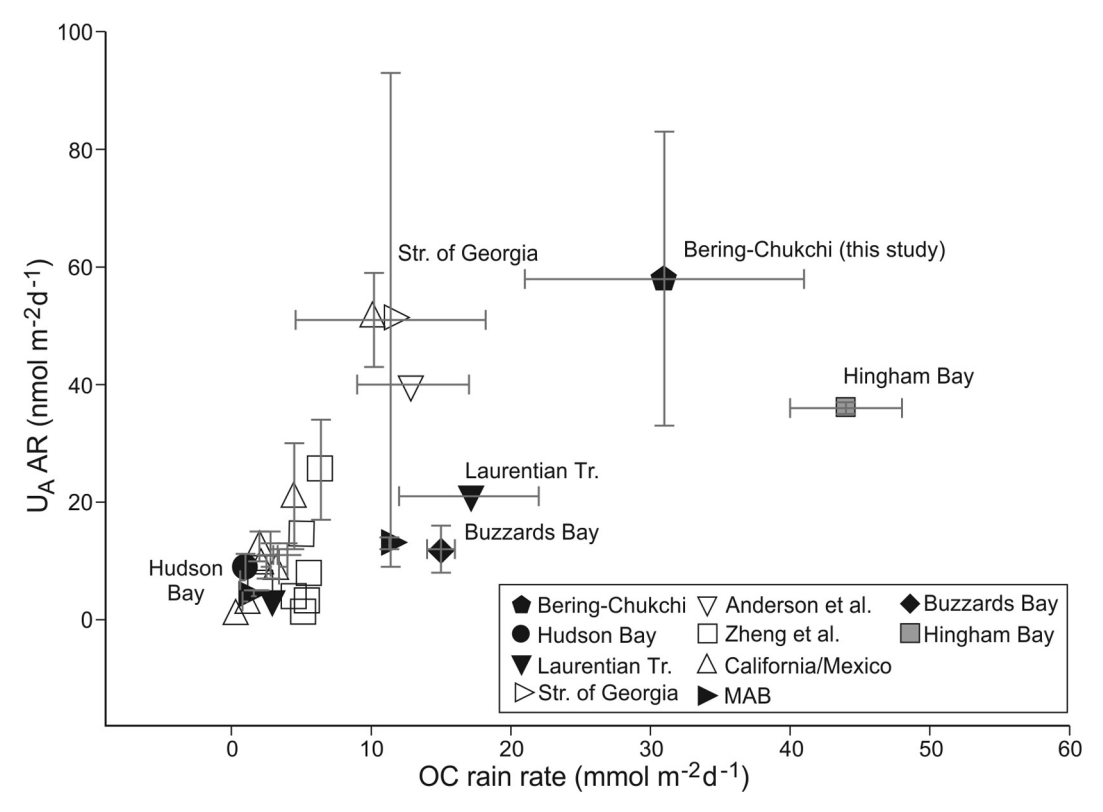


Fig. 12. Authigenic U accumulation rates plotted against organic carbon (OC) rain rates for the Bering–Chukchi shelves and other locations in the global ocean. Data include those of this study, together with those compiled in Table 8 in Morford et al. (2009a), and some additional recent results for Hudson Bay (Kuzyk et al., 2011) and the Strait of Georgia (Macdonald et al., 2008). In keeping with Fig. 6c in Morford et al. (2009a), we have plotted data from locations with low bottom water O_2 levels ($<150 \mu M$) with open symbols and data from locations with high bottom water O_2 levels ($>150 \mu M$) with closed symbols.

those in other locations, including Buzzards Bay and Hingham Bay (Fig. 12) (Morford et al., 2007, 2009a,b). Perhaps the bioturbation and/or bioirrigation is not as intense because of differences in the macrobenthos community, or perhaps the low porosity of the Bering–Chukchi shelf sediments (averaging 0.62–0.77, Table 1) reduces the impact of bioirrigation, compared to locations with fine-grained sediments.

5.5. Implications for estimating the importance of the Arctic for marine budgets of S, Mo, Cd, U, and Re

Accumulation rates of Mo_A, Cd_A, and U_A in sediments have been determined at several locations along both the Pacific (Morford and Emerson, 1999; Nameroff et al., 2002; Zheng et al., 2002b; McManus et al., 2005; Morford et al., 2005; Macdonald et al., 2008) and Atlantic (Sundby et al., 2004; Morford et al., 2007) margins of North America and in the Arctic marginal sea Hudson Bay (Kuzyk et al., 2011). However, none of these studies has included sites along the continental margin of the Arctic Ocean, despite its vastness and potential for future change. The Arctic margin data also contribute new information about redox element accumulation in sediments underlying well-oxygenated bottom waters, which is generally scarce.

Our data reveal considerable spatial variability in accumulation rates of redox-sensitive elements for sediments along the NAAM margin, which will make it challenging to develop accurate estimates of the importance of the Arctic for regional or global marine biogeochemical budgets. For instance, while accumulation rates for Mo_A are negligible in the Canadian Archipelago, Beaufort Shelf, Davis Strait, the average rates in the Chukchi Shelf $(\sim 0.82 \, \mu g \, cm^{-2} \, yr^{-1})$ are comparable to those in other productive margin areas around the world. This variation implies that accumulation rates in one region ought not to be applied to other regions. Another complication is variation within regions, in particular Barrow Canyon, where the nature of the variation is somewhat unexpected (i.e., higher authigenic accumulation rates at the deeper (599 m) BC4 site, compared to the shallow (186 m) BC3 site). In the Beaufort Shelf, the variation is as expected, with higher accumulation rates at the shallowest site (CG1). In the Canadian Archipelago, the most westerly cores (QM1 and VS1) have slightly higher authigenic element accumulation rates than all the cores further east, while in Davis Strait, the opposite spatial pattern is observed (the most easterly site (DS5), which is on the Greenland Shelf, has higher accumulation rates than the more westerly sites on the Baffin Shelf). Considering the complex bathymetry and oceanography of the regions considered here, this small amount of variation within regions is not surprising.

6. CONCLUSIONS

Distributions of Mn, total S and reduced inorganic S along the NAAM demonstrate regional organization

implying strong labile OC flux and carbon turnover in the sediments in the Bering-Chukchi Shelves, lower aerobic OC turnover in Barrow Canyon and Lancaster Sound, and deep O₂ penetration and much lower OC turnover in the Beaufort Shelf, Canadian Archipelago, and Davis Strait. Authigenic Re, Cd, and U enrichments occur in more than 80% of the studied cores in spite of weakly reducing conditions in many of them. Significant authigenic Mo enrichment is limited to the more strongly sulphidic conditions developed in sediments in the Bering-Chukchi shelves, Barrow Canyon, and Lancaster Sound.

Consistent with the wide variation in sedimentary reducing conditions, accumulation rates of S_A, Mo_A, Cd_A, Re_A, and U_A, estimated from sediment accumulation rates in the cores and authigenic concentrations in deep sediment sections (>30 cm), strongly vary with region along the NAAM. Strong relationships between the accumulation rates and vertical carbon flux, estimated from regional primary production values and water depth at the coring sites, indicate that the primary driver in the regional patterns is variation in supply of labile carbon to the seabed. Very high primary production combined with shallow water (average 64 m) drive high rates of authigenic trace element accumulation in sediments in the Bering-Chukchi shelves, high to moderate production combined with deep water (average 610 m) drive moderate rates of authigenic trace element accumulation in sediments in Lancaster Sound, and low to very low production combined with moderate water depths (average 380 m) drive low rates of authigenic trace element accumulation in sediments in the Beaufort Shelf, Davis Strait and Canadian Archipelago. After accounting for the influence of carbon flux, MoA accumulation rates show a significant relationship with vascular plant input to the sediments. We conclude from this result that terrestrial organic matter, in addition to marine OM, contributes to supporting metabolism in Arctic margin sediments. Overall, comparison of accumulation rates among the various regions along this margin and with rates reported for other oceans suggest that the broad and shallow shelf of the Chukchi Sea, which has high productivity sustained by imported nutrients, contributes disproportionately to global biogeochemical cycles for these redox elements.

ACKNOWLEDGEMENTS

We gratefully acknowledge the Canadian IPY Program and the Natural Sciences and Engineering Research Council of Canada for their support to collect cores during the International Polar Year (2007–2008). We thank the Captains and crews of the Canadian Coast Guard Ships Wilfrid Laurier (July 2007) and Louis S. St. Laurent (July 2008). We also thank S. Jobidon for support in the laboratory, D. Dubien for technical assistance at sea, L. Rancourt for research assistance and A. Laberge and P. Kimber for drafting/editing the diagrams. Financial support from the Natural Sciences and Engineering Research Council of Canada and specifically the Canada Excellence Research Chair Program of NSERC are gratefully acknowledged. Finally, we wish to express our thanks to three anonymous reviewers and Timothy J. Shaw (Associate Editor), whose comments greatly improved the final version of the manuscript.

APPENDIX A. SUPPLEMENTARY DATA

Supplementary data associated with this article can be found, in the online version, at http://dx.doi.org/10.1016/j.gca.2016.12.015.

REFERENCES

- Algeo T. J. and Lyons T. W. (2006) Mo-total organic carbon covariation in modern anoxic marine environments: implications for analysis of paleoredox and paleohydrographic conditions. *Paleoceanography* 21.
- Anderson R. F. (1982) Concentrations, vertical flux, and remineralization of particulate uranium in seawater. Geochim. Cosmochim. Acta 46, 1293–1299.
- Arrigo K. R. et al. (2012) Massive phytoplankton blooms under Arctic sea ice. Science 336, 1408.
- Arrigo K. R., van Dijken G. and Pabi S. (2008) Impact of a shrinking Arctic ice cover on marine primary production. *Geophys. Res. Lett.* 35, L19603.
- Baskaran M. and Naidu A. S. (1995) ²¹⁰Pb-derived chronology and the fluxes of ²¹⁰Pb and ¹³⁷Cs isotopes into continental shelf sediments, East Chukchi Sea, Alaskan Arctic. *Geochim. Cosmochim. Acta* **59**, 4435–4448.
- Berger G. W., Fischer K., Lai C. and Wu G. (1987) *Ocean Productivity and Organic Carbon Flux. Part 1. Overview and Maps of Primary Production and Export Production.* University of California, San Diego, p. 67.
- Berner R. A. (1970) Sedimentary pyrite formation. *Am. J. Sci.* **268**, 1–23.
- Berner R. A. (1982) Burial of organic carbon and pyrite sulfur in the modern ocean; its geochemical and environmental significance. *Am. J. Sci.* **282**, 451–473.
- Berner R. A. (1984) Sedimentary pyrite formation: an update. *Geochim. Cosmochim. Acta* 48, 605-615.
- Bishop J. K. B. (1989) Regional extremes in particulate matter composition and flux: effects on the chemistry of the ocean interior. In *Productivity of the Ocean: Present and Past* (eds. W. H. Berger, V. S. Smetacek and G. Wefer). J. Wiley & Sons Limited, Dahlem, pp. 117–137.
- Böning P., Brumsack H.-J., Böttcher M. E., Schnetger B., Kriete C., Kallmeyer J. and Borchers S. L. (2004) Geochemistry of Peruvian near-surface sediments. *Geochim. Cosmochim. Acta* 68, 4429–4451.
- Borchers S. L., Schnetger B., Böning P. and Brumsack H. J. (2005) Geochemical signatures of the Namibian diatom belt: perennial upwelling and intermittent anoxia. *Geochem. Geophys. Geosyst.*.
- Bruland K. W. and Franks R. P. (1983) Mn, Ni, Cu, Zn, and Cd in the western North Atlantic. In *Trace Metals in Seawater* (eds. C. S. Wong, E. A. Boyle, K. W. Bruland, J. D. Burton and E. D. Goldberg). Plenum Press, New York, pp. 395–414.
- Burdige D. J. (2005) Burial of terrestrial organic matter in marine sediments: a re-assessment. Global Biogeochem. Cycles 19, GB4011.
- Cai P., Rutgers van der Loeff M., Stimac I., Nöthig E. M., Lepore K. and Moran S. B. (2010) Low export flux of particulate organic carbon in the central Arctic Ocean as revealed by ²³⁴Th:²³⁸U disequilibrium. *J. Geophys. Res.: Oceans* 115, C10037.
- Cai W.-J. and Sayles F. L. (1996) Oxygen penetration depths and fluxes in marine sediments. *Mar. Chem.* **52**, 123–131.
- Calvert S. E. and Pedersen T. F. (1993) Geochemistry of recent oxic and anoxic marine sediments: implications for the geological record. *Mar. Geol.* 113, 67–88.

- Canfield D. E. (1993) Pathways of organic carbon oxidation in three continental margin sediments. *Mar. Geol.* 113, 27–40.
- Canfield D. E., Raiswell R., Westrich J. T., Reaves C. M. and Bener R. A. (1986) The use of chromium reduction in the analysis of reduced sulfur in sediments and shales. *Chem. Geol.* 54, 149–155.
- Carmack E. C. and Wassman P. (2006) Food webs and physical-biological coupling on pan-Arctic shelves: unifying concepts and comprehensive perspectives. *Prog. Oceanogr.* 71, 446–477.
- Carmack E. C., Barber D., Christensen J. P., Macdonald R. W., Rudels B. and Sakshaug E. (2006) Climate variability and physical forcing of the food webs and the carbon budget on panArctic shelves. *Prog. Oceanogr.* 71, 145–181.
- Carmack E. C., McLaughlin F. A., Vagle S., Melling H. and Williams W. J. (2010) Structures and property distributions in the three oceans surrounding Canada in 2007: a basis for a long-term ocean climate monitoring strategy. *Atmos. Ocean* 48, 211–224.
- Chaillou G., Anschutz P., Lavaux G., Schäfer J. and Blanc G. (2002) The distribution of Mo, U, and Cd in relation to major redox species in muddy sediments of the Bay of Biscay. *Mar. Chem.* **80**, 41–59.
- Chappaz A., Gobeil C. and Tessier A. (2008) Sequestration mechanisms and anthropogenic inputs of rhenium in sediments from Eastern Canada lakes. *Geochim. Cosmochim. Acta* 72, 6027–6036.
- Chappaz A., Lyons T. W., Gregory D. D., Reinhard C. T., Gill B. C., Li C. and Large R. R. (2014) Does pyrite act as an important host for molybdenum in modern and ancient euxinic sediments? *Geochim. Cosmochim. Acta* 126, 112–122.
- Chen C.-T. A., Liu K. K. and Macdonald R. (2003) Continental margin exchanges. In *Ocean Biogeochemistry: The Role of the Ocean Carbon Cycle in Global Change* (ed. M. J. R. Fasham). Springer, Berlin, pp. 53–97 (Chapter 3).
- Cline J. D. (1969) Spectrophotometric determination of hydrogen sulfide in natural waters. *Limnol. Oceanogr.* 14, 454–458.
- Clough L. M., Ambrose W. G. J., Cochran J. K., Barnes C., Renaud P. E. and Aller R. C. (1997) Infaunal density, biomass and bioturbation in the sediments of the Arctic Ocean. *Deep Sea Res. II* 44, 1683–1704.
- Cochran J. K., Carey A. E., Sholkovitz E. R. and Suprenant L. D. (1986) The geochemistry of uranium and thorium in coastal marine sediments and sediment porewaters. *Geochim. Cos-mochim. Acta* 50, 663–680.
- Crusius J. and Thomson J. (2000) Comparative behavior of authigenic Re, Mo and U during reoxidation and subsequent long-term burial in marine sediments. *Geochim. Cosmochim. Acta* **64**, 2233–2243.
- Crusius J. and Thomson J. (2003) Mobility of authigenic rhenium, silver, and selenium during postdepositional oxidation in marine sediments. *Geochim. Cosmochim. Acta* **67**, 265–273.
- Crusius J., Calvert S., Pedersen T. and Sage D. (1996) Rhenium and molybdenum enrichments in sediments as indicators of oxic, suboxic and sulfidic conditions of deposition. *Earth Planet. Sci. Lett.* **145**, 65–78.
- Cuny J., Rhines P. B. and Kwok R. (2005) Davis Strait volume, freshwater and heat fluxes. *Deep Sea Res. I* **52**, 519–542.
- Dahl T. W., Chappaz A., Fitts J. P. and Lyons T. W. (2013) Molybdenum reduction in a sulfidic lake: evidence from X-ray absorption fine-structure spectroscopy and implications for the Mo paleoproxy. *Geochim. Cosmochim. Acta* 103, 213–231.
- Darby D. A., Ortiz J., Polyak L., Lund S., Jakobsson M. and Woodgate R. A. (2009) The role of currents and sea ice in both slowly deposited central Arctic and rapidly deposited Chukchi-Alaskan margin sediments. Global Planet. Change 68, 58–72.

- Doney S. C., Ruckelshaus M., Emmett Duffy J., Barry J. P., Chan F., English C. A., Galindo H. M., Grebmeier J. M., Hollowed A. B., Knowlton N., Polovina J., Rabalais N. N., Sydeman W. J. and Talley L. D. (2012) Climate change impacts on marine ecosystems. *Annu. Rev. Mar. Sci.* 4, 11–37.
- Dunk R. M., Mills R. A. and Jenkins W. J. (2002) A reevaluation of the oceanic uranium budget for the Holocene. *Chem. Geol.* 190, 45–67.
- Dunton K. H., Goodall J. L., Schonberg S. V., Grebmeier J. M. and Maidment D. R. (2005) Multi-decadal synthesis of benthic-pelagic coupling in the western arctic: Role of cross-shelf advective processes. *Deep Sea Res. Part II* 52, 3462–3477.
- Erickson B. E. and Helz G. R. (2000) Molybdenum (VI) speciation in sulfidic waters. Stability and lability of thiomolybdates. *Geochim. Cosmochim. Acta* **64.** 1149–1158.
- Esch M. E. S., Shull D. H., Devol A. H. and Moran S. B. (2013) Regional patterns of bioturbation and iron and manganese reduction in the sediments of the southeastern Bering Sea. *Deep Sea Res. Part II* **94**, 80–94.
- Esser B. K. and Turekian K. K. (1993) The osmium isotopic composition of the continental crust. *Geochim. Cosmochim. Acta* 57, 3093–3104.
- Froelich P. N., Klinkhammer G. P., Bender M. L., Luedtke N. A., Heath G. R., Cullen D., Dauphin P., Hammond D. E., Hartman B. and Maynard V. (1979) Early oxidation of organic matter in pelagic sediments of the eastern equatorial Atlantic: suboxic diagenesis. *Geochim. Cosmochim. Acta* 43, 1075–1090.
- Gariépy C., Ghaleb B., Hillaire-Marcel C., Mucci A. and Vallières S. (1994) Early diagenetic processes in Labrador Sea sediments: uranium-isotope geochemistry. *Can. J. Earth Sci.* **31**, 28–37.
- Gendron A., Silverberg N., Sundby B. and Lebel J. (1986) Early diagenesis of cadmium and cobalt in sediments of the Laurentian Trough. Geochim. Cosmochim. Acta 50, 741–747.
- Gobeil C., Paton D., McLaughlin F. A., Macdonald R. W., Paquette G., Clermont Y. and Lebeuf M. (1991) Données géochimiques sur les eaux interstitielles et les sédiments de la mer de Beaufort, Rapport Statistique Canadien Sur l'hydrographie et les Sciences océaniques. Fish. Oceans Canada, 1–92.
- Gobeil C., Silverberg N., Sundby B. and Cossa D. (1987) Cadmium diagenesis in Laurentian Trough sediments. Geochim. Cosmochim. Acta 51, 589-596.
- Goñi M. A., O'Connor A., Kuzyk Z. A., Yunker M. B., Gobeil C. and Macdonald R. W. (2013) Distribution and sources of organic matter in surface marine sediments across the North American Arctic margin. J. Geophys. Res. Oceans 118, 1–19.
- Goñi M. A., Yunker M. B., Macdonald R. W. and Eglinton T. I. (2005) The supply and preservation of ancient and modern components of organic carbon in the Canadian Beaufort Shelf of the Arctic Ocean. *Mar. Chem.* 93, 53–73.
- Goñi M. A., Yunker M. B., Macdonald R. W. and Eglinton T. I. (2000) Distribution and sources of organic biomarkers in Arctic sediments from the Mackenzie River and Beaufort Shelf. *Mar. Chem.* 71, 23–51.
- Grebmeier J. M. and Cooper L. W. (1995) Influence of the St. Lawrence Island Polynya upon the Bering Sea benthos. *J. Geophys. Res.: Oceans* **100**, 4439–4460.
- Grebmeier J. M., Cooper L. W., Feder H. M. and Sirenko B. I. (2006) Ecosystem dynamics of the Pacific-influenced Northern Bering and Chukchi Seas in the Amerasian Arctic. *Prog. Oceanogr.* 71, 331–361.
- Guo L., Cai Y., Belzile C. and Macdonald R. (2012) Sources and export fluxes of inorganic and organic carbon and nutrient species from the seasonally ice-covered Yukon River. *Biogeo-chemistry* 107, 187–206.

- Hebert C. E. and Keenleyside K. A. (1995) To normalize or not to normalize? Fat is the question. *Environ. Toxicol. Chem.* 14, 801– 807.
- Helz G. R. and Adelson J. M. (2013) Trace element profiles in sediments as proxies of Dead Zone history; rhenium compared to molybdenum. *Environ. Sci. Technol.* 47, 1257–1264.
- Helz G. R. and Dolor M. K. (2012) What regulates rhenium deposition in euxinic basins? Chem. Geol. 304–305, 131–141.
- Helz G. R., Miller C. V., Charnock J. M., Mosselmans J. F. W., Pattrick R. A. D., Garner C. D. and Vaughan D. J. (1996) Mechanism of molybdenum removal from the sea and its concentration in black shales: EXAFS evidence. *Geochim. Cosmochim. Acta* 60, 3631–3642.
- Horak R. E. A., Whitney H., Shull D. H., Mordy C. W. and Devol A. H. (2013) The role of sediments on the Bering Sea shelf N cycle: insights from measurements of benthic denitrification and benthic DIN fluxes. *Deep Sea Res. Part II* 94, 95–105.
- Hsieh Y. P. and Yang C. H. (1989) Diffusion methods for the determination of reduced inorganic sulfur species in sediments. *Limnol. Oceanogr.* 34, 1126–1130.
- Hsieh Y. P., Chung S. W., Tsau Y. J. and Sue C. T. (2002) Analysis of sulfides in the presence of ferric minerals by diffusion methods. *Chem. Geol.* 182, 195–201.
- Hulth S., Blackburn T. H. and Hall P. O. J. (1994) Arctic sediments (Svalbard): consumption and microdistribution of oxygen. *Mar. Chem.* 46, 293–316.
- IPCC (2013) Summary for Policymakers. In Climate Change 2013: The Physical Science Basis. Contribution of Working Group I to the Fifth Assessment Report of the Intergovernmental Panel on Climate Change (eds. T. F. Stocker, D. Qin, G. -K. Plattner, M. Tignor, S. K. Allen, J. Boschung, A. Nauels, Y. Xia, V. Bex and P.M. Midgley). Cambridge University Press, Cambridge, United Kingdom and New York, NY, USA.
- Jakobsson M. (2002) Hypsometry and volume of the Arctic Ocean and its constituent seas. Geochem. Geophys. Geosyst. 3, 1–18.
- Jeandel C., Peucker-Ehrenbrink B., Jones M. T., Pearce C. R., Oelkers E. H., Godderis Y., Lacan F., Aumont O. and Arsouze T. (2011) Ocean margins: the missing term in oceanic element budgets? EOS Trans. Am. Geophys. Union 92, 217–218.
- Katsev S., Sundby B. and Mucci A. (2006) Modeling vertical excursions of the redox boundary in sediments: application to deep basins of the Arctic Ocean. *Limnol. Oceanogr.* 51, 1581– 1593.
- Klinkhammer G. P. and Palmer M. R. (1991) Uranium in the oceans: where it goes and why. *Geochim. Cosmochim. Acta* 55, 1799–1806.
- Klunder M. B., Bauch D., Laan P., de Baar H. J. W., van Heuven S. and Ober S. (2012) Dissolved iron in the Arctic shelf seas and surface waters of the central Arctic Ocean: impact of Arctic river water and ice-melt. J. Geophys. Res.: Oceans 117, C01027.
- Kostka J. E., Thamdrup B., Glud R. N. and Canfield D. E. (1999) Rates and pathways of carbon oxidation in permanently cold Arctic sediments. *Mar. Ecol. Prog. Ser.* 180, 7–21.
- Kuzyk Z. A., Gobeil C. and Macdonald R. W. (2013) ²¹⁰Pb and ¹³⁷Cs in margin sediments of the Arctic Ocean: controls on boundary scavenging. *Global Biogeochem. Cycles* 27, 422–439.
- Kuzyk Z. A., Macdonald R. W., Stern G. A. and Gobeil C. (2011) Inferences about the modern organic carbon cycle from diagenesis of redox-sensitive elements in Hudson Bay. J. Mar. Syst. 88, 451–462.
- Lantuit H., Overduin P. P. and Wetterich S. (2013) Recent progress regarding permafrost coasts. *Permafrost Periglac. Process.* 24, 120–130.

- Lepore K., Moran S. B. and Smith J. N. (2009) ²¹⁰Pb as a tracer of shelf-basin transport and sediment focusing in the Chukchi Sea. *Deep Sea Res. II* **56**, 1305–1315.
- Little S. H., Vance D., Lyons T. W. and McManus J. (2015) Controls on trace metal authigenic enrichment in reducing sediments: insights from modern oxygen-deficient settings. Am. J. Sci. 315, 77–119.
- Liu K.-K., Atkinson L., Quinones R. and Talaue-McManus L. (2010) Carbon and Nutrient Fluxes in Continental Margins: A Global Synthesis. Springer, Berlin.
- Liu K.-K., Iseki K. and Chao S.-Y. (2000b) Continental margin carbon fluxes. In *The Changing Ocean Carbon Cycle: A Midterm Synthesis of the Joint Global Ocean Flux Study* (eds. R. B. Hanson, H. W. Ducklow and J. G. Field). Cambridge University Press, Cambridge, pp. 187–239.
- Liu K.-K., Atkinson L., Chen C. T. A., Gao S., Hall J., MacDonald R. W., McManus L. T. and Quiñones R. (2000a) Exploring continental margin carbon fluxes on a global scale. EOS Trans. Am. Geophys. Union 81, 641–644.
- Macdonald R. W., Kuzyk Z. A. and Johannessen S. C. (2015a) It is not just about the ice: a geochemical perspective on the changing Arctic Ocean. J. Environ. Stud. Sci. 5, 288–301.
- Macdonald R. W., Kuzyk Z. A. and Johannessen S. C. (2015b) The vulnerability of arctic shelf sediments to climate change. *Environ. Rev.* 23, 461–479.
- Macdonald R. W. and Gobeil C. (2012) Manganese sources and sinks in the Arctic Ocean with reference to periodic enrichments in basin sediments. *Aquat. Geochem.* **18**, 565–591.
- Macdonald R. W., Anderson L. G., Christensen J. P., Miller L. A., Semiletov I. P. and Stein R. (2010) The Arctic Ocean. In *Carbon and Nutrient Fluxes in Continental Margins: A Global Synthesis* (eds. K. K. Liu, L. Atkinson, R. Quinones and L. Talaue-McManus). Springer, Berlin, pp. 291–303 (chapter 6.2).
- Macdonald R. W., Johannessen S. C., Gobeil C., Wright C., Burd B., van Roodselaar A. and Pedersen T. F. (2008) Sediment redox tracers in Strait of Georgia sediments can they inform us of the loadings of organic carbon from municipal wastewater? *Mar. Environ. Res.* 66(Suppl. 1), S39–S48.
- Macdonald R. W., Solomon S. M., Cranston R. E., Welch H. E., Yunker M. B. and Gobeil C. (1998) A sediment and organic carbon budget for the Canadian Beaufort Shelf. *Mar. Geol.* 144, 255–273
- McGuire A. D., Anderson L. G., Christensen T. R., Dallimore S., Guo L., Hayes D. J., Heimann M., Lorenson T. D., Macdonald R. W. and Roulet N. (2009) Sensitivity of the carbon cycle in the Arctic to climate change. *Ecol. Monogr.* 79, 523–555.
- McLennan S. M. (2001) Relationships between the trace element composition of sedimentary rocks and upper continental crust. *Geochem. Geophys. Geosyst.* 2, 1021.
- McManus D. A., Kelley J. C. and Creager J. S. (1969) Continental shelf sedimentation in an Arctic environment. GSA Bull. 80, 1961–1984.
- McManus J., Berelson W. M., Klinkhammer G. P., Hammond D. E. and Holm C. (2005) Authigenic uranium: relationship to oxygen penetration depth and organic carbon rain. *Geochim. Cosmochim. Acta* 69, 95–108.
- McManus J., Berelson W. M., Severmann S., Poulson R. L., Hammond D. E., Klinkhammer G. P. and Holm C. (2006) Molybdenum and uranium geochemistry in continental margin sediments: paleoproxy potential. *Geochim. Cosmochim. Acta* 70, 4643–4662.
- Moran S. B., Shen C.-C., Edwards R. L., Edmonds H. N., Scholten J. C., Smith J. N. and Ku T.-L. (2005) ²³¹Pa and ²³⁰Th in surface sediments of the Arctic Ocean: implications for ²³¹Pa/²³⁰Th fractionation, boundary scavenging, and advective transport. *Earth Planet. Sci. Lett.* **234**, 235–248.

- Morel F. M. M. and Malcom E. G. (2005) The biogeochemistry of cadmium. In *Metal Ions in Biological Systems: Biogeochemical Cycles of Elements* (eds. S. Astrid, H. Sigel and R. K. O. Sigel). Taylor & Francis Group, Boca Raton, FL, pp. 195–219.
- Morford J. L. and Emerson S. R. (1999) The geochemistry of redox sensitive trace metals in sediments. *Geochim. Cosmochim. Acta* 63, 1735–1750.
- Morford J. L., Martin W. R. and Carney C. M. (2009a) Uranium diagenesis in sediments underlying bottom waters with high oxygen content. *Geochim. Cosmochim. Acta* 73, 2920–2937.
- Morford J. L., Martin W. R. and Carney C. M. (2012) Rhenium geochemical cycling: insights from continental margins. *Chem. Geol.* 324–325, 73–86.
- Morford J. L., Emerson S. R., Breckel E. J. and Kim S. H. (2005) Diagenesis of oxyanions (V, U, Re, and Mo) in pore waters and sediments from a continental margin. *Geochim. Cosmochim. Acta* **69**, 5021–5032.
- Morford J. L., Martin W. R., Francois R. and Carney C. M. (2009b) A model for uranium, rhenium, and molybdenum diagenesis in marine sediments based on results from coastal locations. *Geochim. Cosmochim. Acta* 73, 2938–2960.
- Morford J. L., Martin W. R., Kalnejais L. H., Francois R., Bothner M. and Karle I.-M. (2007) Insights on geochemical cycling of U, Re and Mo from seasonal sampling in Boston Harbor, Massachusetts, USA. *Geochim. Cosmochim. Acta* 71, 895–917.
- Nameroff T. J., Balistrieri L. S. and Murray J. W. (2002) Suboxic trace metal geochemistry in the eastern tropical North Pacific. *Geochim. Cosmochim. Acta* 66, 1139–1158.
- Nickel M., Vandieken V., Bruchert V. and Jørgensen B. B. (2008) Microbial Mn(IV) and Fe(III) reduction in northern Barents Sea sediments under different conditions of ice cover and organic carbon deposition. *Deep Sea Res. II* 55, 2390–2398.
- O'Brien M. C., Melling H., Pedersen T. F. and Macdonald R. W. (2011) The role of eddies and energetic ocean phenomena in the transport of sediment from shelf to basin in the Arctic. *J. Geophys. Res.* **116**.
- Peucker-Ehrenbrink B. and Jahn B. (2001) Rhenium—osmium isotope systematics and platinum group element concentrations: loess and the upper continental crust. *Geochem. Geophys. Geosyst.* 2, 1061.
- Pickart R. S., Weingartner T. J., Pratt L. J., Zimmermann S. and Torres D. J. (2005) Flow of winter-transformed Pacific water into the Western Arctic. *Deep Sea Res. II* 52, 3175–3198.
- Prahl F. G., Ertel J. R., Goñi M. A., Sparrow M. A. and Eversmeyer B. (1994) Terrestrial organic carbon contributions to sediments on the Washington margin. *Geochim. Cosmochim.* Acta 58, 3035–3048.
- Raiswell R., Tranter M., Benning L. G., Siegert M., De'ath R., Huybrechts P. and Payne T. (2006) Contributions from glacially derived sediment to the global iron (oxyhydr)oxide cycle: implications for iron delivery to the oceans. *Geochim. Cosmochim. Acta* 70, 2765–2780.
- Rosenthal Y., Boyle E. A., Labeyrie L. and Oppo D. (1995a) Glacial enrichments of authigenic Cd and U in subant Arctic sediments: a climatic control on the elements' oceanic budget? *Paleoceanography* **10**, 395–413.
- Rosenthal Y., Lam P., Boyle E. A. and Thomson J. (1995b) Authigenic Cd enrichment in suboxic sediments: precipitation and postdepositional mobility. *Earth Planet. Sci. Lett.* **132**, 99–111
- Rudnick R. L. and Gao (2003) Composition of the continental crust. In *Treatise on Geochemistry*, vol. 3 (ed. R. L. Rudnick). Elsevier, pp. 1–64.
- Sakshaug E. (2004) Primary and secondary production in the Arctic seas. In *The Organic Carbon Cycle in the Arctic Ocean*

- (eds. R. Stein and R. W. Macdonald). Springer, Berlin, pp. 57-81
- Sánchez-García L., Alling V., Pugach S., Vonk J., van Dongen B., Humborg C., Dudarev O., Semiletov I. and Gustafsson Ö. (2011) Inventories and behavior of particulate organic carbon in the Laptev and East Siberian seas. *Global Biogeochem. Cycles* 25. GB2007.
- Scholz F., McManus J. and Sommer S. (2013) The manganese and iron shuttle in a modern euxinic basin and implications for molybdenum cycling at euxinic ocean margins. *Chem. Geol.* 355, 56–68.
- Scott C., Lyons T. W., Bekker A., Shen Y., Poulton S. W., Chu X. and Anbar A. D. (2008) Tracing the stepwise oxygenation of the Proterozoic ocean. *Nature* 452, 456–459.
- Serreze M. C., Holland M. M. and Stroeve J. (2007) Perspectives on the Arctic's shrinking sea-ice cover. *Science* **315**, 1533–1536.
- Shiklomanov I. A. and Shiklomanov A. I. (2003) Climatic change and the dynamics of river runoff into the Arctic Ocean. Water Resour. 30, 593–601.
- Shimmield G. B. and Price N. B. (1986) The behaviour of molybdenum and manganese during early diagenesis—offshore Baja California, Mexico. *Mar. Chem.* 19, 261–280.
- Stein R. and Macdonald R. (2004) *The Organic Carbon Cycle of the Arctic Ocean*. Springer, Berlin.
- Suess E. (1980) Particulate organic carbon flux in the ocean surface productivity and oxygen utilization. *Nature* 288, 260– 263.
- Sundby B., Martinez P. and Gobeil C. (2004) Comparative geochemistry of cadmium, rhenium, uranium, and molybdenum in continental margin sediments. *Geochim. Cosmochim.* Acta 68, 2485–2493.
- Taylor S. R. and McLennan S. M. (1986) The chemical composition of the Archaean crust. Geol. Soc. Lond. Special Publ. 24, 173–178.
- Thomson J., Nixon S., Croudace I. W., Pedersen T. F., Brown L., Cook G. T. and MacKenzie A. B. (2001) Redox-sensitive element uptake in north-east Atlantic Ocean sediments (Benthic Boundary Layer Experiment sites). *Earth Planet. Sci. Lett.* 184, 535–547.

- Tribovillard N., Algeo T. J., Lyons T. and Riboulleau A. (2006) Trace metals as paleoredox and paleoproductivity proxies: an update. *Chem. Geol.* **232**, 12–32.
- Turekian K. K. and Wedepohl K. H. (1961) Distribution of the elements in some major units of the earth's crust. *Bull. Geol. Soc. Am.* **72**, 175–191.
- Vandieken V., Nickel M. and Jørgensen B. B. (2006) Carbon mineralization in Arctic sediments northeast of Svalbard: Mn (IV) and Fe(III) reduction as principal anaerobic respiratory pathways. *Mar. Ecol. Prog. Ser.* 322, 15–27.
- Vigier N., Bourdon B., Turner S. and Allègre C. J. (2001) Erosion timescales derived from U-decay series measurements in rivers. *Earth Planet. Sci. Lett.* 193, 549–563.
- Vonk J. E., Sanchez-Garcia L., van Dongen B. E., Alling V., Kosmach D., Charkin A., Semiletov I. P., Dudarev O. V., Shakhova N., Roos P., Eglinton T. I., Andersson A. and Gustafsson O. (2012) Activation of old carbon by erosion of coastal and subsea permafrost in Arctic Siberia. *Nature* 489, 137–140.
- Walsh J. E., Overland J. E., Groisman P. Y. and Rudolf B. (2011) Ongoing climate change in the Arctic. *Ambio* 40, 6–16.
- Wedepohl K. H. (1995) The composition of the continental crust. *Geochim. Cosmochim. Acta* **59**, 1217–1232.
- Weingartner T. J., Aagaard K., Woodgate R. A., Danielson S., Sasaki Y. and Cavalieri D. (2005) Circulation on the north central Chukchi Sea shelf. *Deep Sea Res. II* 52, 3150–3171.
- Williams W. J., Melling H., Carmack E. C. and Ingram R. G. (2008) Kugmallit Valley as a conduit for cross-shelf exchange on the Mackenzie shelf in the Beaufort Sea. J. Geophys. Res. 113.
- Zheng Y., Anderson R. F., van Geen A. and Fleisher M. Q. (2002a) Preservation of particulate non-lithogenic uranium in marine sediments. *Geochim. Cosmochim. Acta* **66**, 3085–3092.
- Zheng Y., Anderson R. F., van Geen A. and Fleisher M. Q. (2002b) Remobilization of authigenic uranium in marine sediments by bioturbation. *Geochim. Cosmochim. Acta* 66, 1759–1772.

Associate editor: Timothy J. Shaw